August | 2012

Utilizing RF Resonators to Monitor States of Hydration on the Skin's Surface in Real-Time

Beibhinn O'Donoghue – Master's Thesis

Table of Contents

Acknowledgements **4**

Abstract **5**

1.Introduction **6**
- **1.1 Dehydration Overview** **6**
- **1.2 Current State of Dehydration Detection** **7**
  - 1.2.1 Weight Monitoring 7
  - 1.2.2 Urine Analysis 7
  - 1.2.3 Sweat Patches 7
- **1.3 Physiology of Dehydration** **8**
  - 1.3.1 Ions Involved 9
  - 1.3.2 Sweat Rates 10
- **1.4 RF Background** **10**
  - 1.4.1 What is an RF resonator? 11
  - 1.4.2 Characteristics of RF Resonator Response 12
- **1.5 Measuring the RF Response** **13**
  - 1.5.1 Parameters of RF Response 13
  - 1.5.2 S-Parameters: Transmission and Reflection 13
  - 1.5.3 Logarithmic Magnitude Plot 14
  - 1.5.4 Smith Chart 15
- **1.6 RF Resonator Design Considerations** **15**
  - 1.6.1 Wireless vs. Wired Transmission 16
  - 1.6.2 ISM Bands 17
  - 1.6.3 Read Range 17
  - 1.6.4 NFC vs. Bluetooth 18
  - 1.6.5 Active vs. Passive 19
- **1.7 Prior Work** **19**

2.Methods & Materials **21**
- **2.1 Silk processing** **21**
  - 2.1.1 Silk Sponges 22
- **2.2 Measurement Instruments** **22**
  - 2.2.1 Network Analyzer 22
  - 2.2.2 Parameters Measured 23
  - 2.2.3 Mobile Device - Android 24
- **2.3 RF Resonators** **24**
  - 2.3.1 Commercially available RFID tags 24
  - 2.3.2 Fabricated RF Resonators 24
- **2.4 Sweat Patch Design** **25**
  - 2.4.1 Absorbing Material 26
  - 2.4.2 Insulating Material 26
  - 2.4.3 Shadow Masked RF Resonators 27
  - 2.4.4 Sweat Patch Prototype 28
  - 2.4.5 Sweat Simulator 28
- **2.5 Performance Analysis** **29**
  - 2.5.1 Analytes Tested 29
  - 2.5.2 Analyte Detection Experiments 30
  - 2.5.3 Volume Detection Experiments 30

2.5.4 Signal Strength Experiments 30
2.5.5 Dehydration Experiments 31
2.5.6 Sweat Collection Experiments 31

3.Results 32
3.1 Volume Detection Experiments 32
3.2 Analyte Detection Experiments 33
3.2.1 Reflection Measurements 33
3.2.2 Transmission Measurements 36
3.3 Signal Strength Experiments 37
3.3.1 Positional Dependence 37
3.3.2 Read Distance Testing 39
3.3.3 Roast Beef slice experiments 39
3.4 Dehydration Experiments 41
3.4.1 Silk Sponge Dehydration 41
3.4.2 Beef Tenderloin Dehydration 43
3.5 Sweat Collection Experiments 45
3.5.1 Initial Human Testing 45
3.5.2 Sweat Patch Prototype Testing – Sweat Simulator 45
3.6 Android App 46
3.7 Fabricated Resonators 46
3.8 Water Quality Testing 47

4.Discussion 49
4.1 RF Resonator Performance 49
4.1.1 Sweat Volume Detection 49
4.1.2 Sweat Composition Detection 49
4.2 Android App Development 50
4.3 Future Directions 51
4.3.1 Integration with Mobile Devices 51
4.3.2 Multi-Sensor Array Network 52
4.3.3 Water Quality Monitoring 52

References 54

Acknowledgements

I would like to start by acknowledging my thesis committee members: Dr. David Kaplan, Dr. Hu Tao, and especially my advisor Dr. Fiorenzo Omenetto. Thank you all for agreeing to be a part of my thesis effort and shaping my experiences along the way. As my advisor, Dr. Omenetto has provided both project and people related guidance and direction throughout, for which I am grateful. It was also nice to share this thesis process with someone who has an even greater appreciation for all things sporting than I do.

I would also like to acknowledge others within the Tufts Biomedical Engineering department faculty and staff, including (but not limited to): Dr. Mark Cronin-Golomb for helping to convince me to become a double Jumbo; Dr. Sergio Fantini for teaching a great class and making it easy to be a TA; and Milva Ricci for keeping the SS Scitech afloat.

There are a number of members of the Omenetto lab group that have lended assistance in various forms, including (but not limited to): Dr. Hu Tao, for always having the right nugget of knowledge at the time it was most needed; Miaomiao Yang, for knowledge of EE concepts and giving confidence that I was on the right path; Mark Paquette for battling with the newly acquired milling machine; and Katie Martinick for help sputter coating samples.

Finally, to my friends – thanks for putting up with my absence at some events over the last two years, I'm ready to make up for it and can monitor dehydration in the process. A very big thanks to my Mom, Dad and soon-to-be Dr. Brother – you've played a large part in shaping who I am today and it's been to my great benefit. And to my fiancée (!), I've mastered a lot of skills I can translate to planning a really great wedding.

Abstract

Dehydration is a physiological side effect of exertion that affects everyone to some degree and can be remedied easily. However, when the rate of dehydration is not monitored appropriately, serious physical consequences can occur. Studies have shown that sweat loss amounting to 2-3% of body weight leads to impaired thermoregulation and increased muscle fatigue, while 5-6% can lead to heat stroke and even coma.

The development of a real-time biosensor to monitor the conditions on the skin's surface and relay that information to a qualified physician or trainer is tantamount to effectively monitoring dehydration. As the details of this work outline, efforts are under way to combine an RF resonator and a variety of biocompatible materials to realize the application of a real-time hydration sensor.

By exploiting and measuring the electrical characteristics of the RF resonator, changes in the surrounding environment will alter the resonator's response. These include changes in both the dielectric and conductivity of the material in contact with the resonator. This is particularly useful for monitoring the hydration level on the surface of the skin, as both the amount of sweat and salt content of sweat vary as dehydration occurs.

Silkworm silk is explored as an absorbing layer, as it can be purified and manipulated to form a porous sponge-like form factor. Alternately, cellulose materials currently used in sweat patches can be utilized in the overall sweat patch design. Whether made of cellulose or silk, this absorbing layer is incorporated with the RF resonator to wick sweat at the skin's surface and bring it in contact with the interrogating resonator. Initial test show that changes in physiologically relevant sweat concentrations can be detected by the RF resonator, showing great promise for this biocompatible real-time, non-invasive hydration monitoring biosensor.

1.Introduction

The genesis of this project was an effort to create a Radio Frequency (RF) sensor that would detect changes in the levels of two hormones in saliva. Cortisol and testosterone both play an integral role in determining how stressed the human body is during any physiological endeavor. By comparing the ratio of the muscle-building testosterone and cortisol – which breaks down muscle – a picture of the body's performance response to exercise (Maso, 2004) appears. A non-invasive, real-time approach was attempted to monitor the rates of the two hormones, as existing techniques involve lab processing time that can take days (Raff, 2003). The notion of using RF resonators was proposed, as the resonators are susceptible to changes in their surrounding environment. Testosterone is considered a Schedule II controlled substance and is therefore harder to obtain, so cortisol was instead used for initial testing. Initial tests concluded that the concentrations of cortisol present in saliva were too small to detect with the RF resonators. However, in preparing the powder form of cortisol in a solution to test with the resonators an interesting trend emerged. A shift in resonant frequency was observed as aqueous solution – in which the cortisol was suspended – came in contact with the resonator. The focus of the project then shifted to developing a real-time, wireless, non-invasive dehydration sensor by incorporating an RF resonator.

1.1 Dehydration Overview

Dehydration is a physiological response that everyone has experienced to some degree. However, if proper rehydration doesn't occur, serious side effects can occur – ranging from muscle cramping to heat stroke and death. Sweat is a response to the physical exertion, and sweat loss becomes a marker of what toll the body is taking when fluids aren't replenished. Table 1 shows what percentage of overall body loss to sweat can mean for the physical performance.

Body Water Loss	Effects
0.5%	Increased strain on heart
1.0%	Reduced aerobic endurance
3.0%	Reduced muscular endurance
4.0%	Reduced muscle strength, fine motor skills; heat cramps
5.0%	Heat exhaustion; cramping; fatigue; reduced mental capacity
6.0%	Heatstroke; coma

Table 1: Physiological Effects of Sweat Loss as Percentage of Body Weight (Ivy, 2004)

Alarmingly, a 6% loss of body mass as sweat can lead to heat stroke or even coma (Ivy, 2004). The need to monitor sweat rates and corresponding dehydration in real-time is not just to ensure peak performance in athletes, but can be extended to other factions of the population that suffer the ill effects of dehydration. These

include members of the military and the elderly, with the latter at increased risk due to a suppression of thirst response as the body ages (Lavizzo-Mourey, 1987).

1.2 Current State of Dehydration Detection

There are a number of methods currently undertaken to monitor the state of dehydration in the body, some technical and others rudimentary. Sometimes a combination of individual techniques is used to try to provide a complete physiological picture of dehydration.

1.2.1 Weight Monitoring

Table 1 demonstrates one method employed to determine states of dehydration, namely the monitoring of body weight gain and loss. Body weight is measured before and after exercise, and any loss of biomass or gain of fluids is accounted for in the calculation of overall weight loss. The weight measurements are also made with minimal clothing on, to ensure that any sweat lost to clothing is not erroneously part of the weight measurement. With the weight before and after, any loss in weight is assumed to be due to sweat loss and can be calculated as a percentage of total body weight. Every pound of body weight lost can be correlated to 450mL of sweat loss through dehydration (Coyle, 1994). This corresponds to a conversion factor of 453.59 grams in an avoirdupois pound. Though a useful metric to determine how much sweat was lost during exercise, it is dependent upon making exact measurements of biomass lost and fluids acquired throughout exercise, which is not always feasible.

1.2.2 Urine Analysis

As the body dehydrates, the composition of urine will change accordingly. A number of quantifiable measures of urine are taken to determine correlated states of hydration such as urine color, specific gravity and osmolality (Armstrong, 1998). Since determination of urine color is the indicator that doesn't necessarily require processing of the sample, urine color charts are utilized to provide a quick diagnostic of dehydration – with darker colored urine demonstrating a more dehydrated individual (Mentes, 2006). However, the analysis of urine color is somewhat subjective, and other factors can affect the color of urine, such as certain dietary or medicinal ingested substances (Simerville, 2005). While some reviewers laud the ability of urine analysis to indicate hydration states (Armstrong, 1998), others call into question the validity of the practice (Kovacs, 1999). Overall, the strength of urine analysis as a hydration diagnostic meets with mixed results and isn't a standalone method to determine the hydration state in the body.

1.2.3 Sweat Patches

Some trainers supplement weight monitoring or urine analysis with the use of sweat patches to keep track of the hydration of their athletes (Yeargin, 2010). Sweat patches can be placed in various locations, including the forearm, back, thigh, and forehead and after exercise are sent to a laboratory for analysis (Baker, 2009). The ability to monitor electrolyte levels in sweat as well as the overall amount of sweat lost over the course of exercise provides important information about

dehydration (Baker, 2009). While the sweat patches are effective in collecting relevant information about sweat that correlates to overall hydration states, the process is hampered by the need to send sweat patches to laboratory and awaiting the results.

Table 2 highlights the benefits and drawbacks of each of the three main hydration monitoring methods, and emphasizes the need for a real-time, non-invasive sensing solution.

Method	Fast?	Quantifiable?	Reliable Alone?
Urine Analysis	Yes	No	No
Sweat Patches	No	Yes	Yes
Weight monitoring	Yes	Yes	No

Table 2: Analysis of current hydration monitoring methods

Analysis of the methods also provides an insight into what parameters of the physiological response to dehydration are useful. The ability to monitor both the composition of relevant ions in sweat, as well as the overall amount of sweat collected over the course of exercise – or over the course of the day for elderly patients – would afford the ability to monitor the hydration state in real-time.

1.3 Physiology of Dehydration

In order to effectively assess the level of hydration through sweat analysis, it's important to understand the mechanism of dehydration and what the physiological hallmarks of dehydration are in sweat. Figure 1 demonstrates at a high-level the events that occur within the body in response to physical exertion.

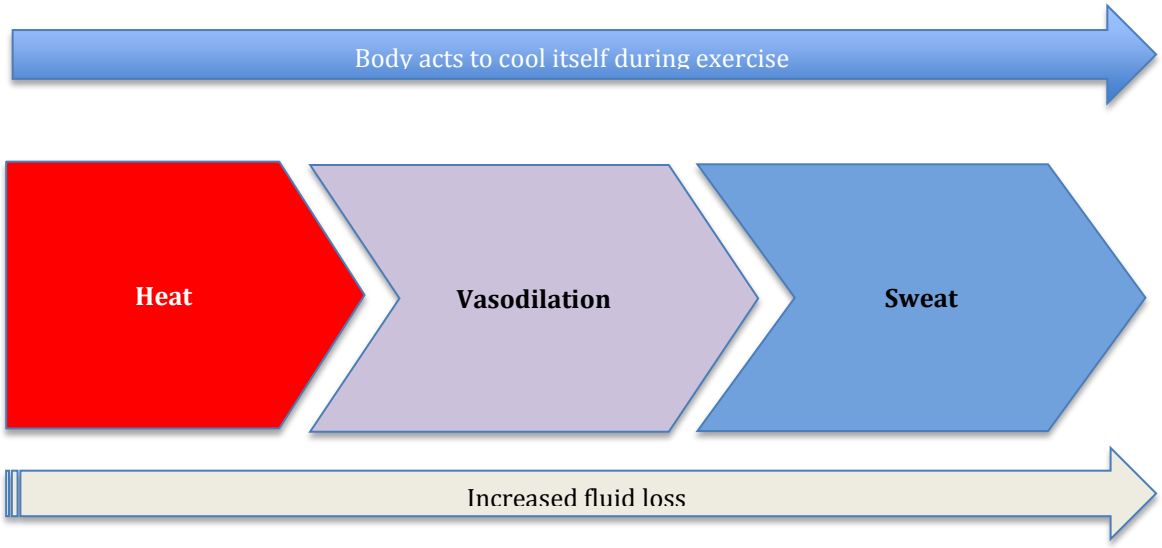

Figure 1: Physiological response to exercise or physical exertion

As the body exercises, the body core temperature rises which in turn leads to a cascade of events that include vasodilation of blood vessels and eventually sweating as the body acts to cool itself (Peak Performance website, 2011). Fluid lost

due to sweat needs to be replenished in order to ensure that the body can continue to function optimally, otherwise dehydration occurs. Without appropriate fluid intake, the effects of dehydration start to take place – overtaxing the cardiovascular system as the overall blood volume decreases (Peak Performance website, 2011). Both sweat composition and overall sweat loss are parameters that need to be measured to determine when and how much fluid replenishment should occur.

1.3.1 Ions Involved

When analyzing sweat composition, sodium and potassium are the most commonly monitored ions, as well as magnesium in some instances (Palaciosa, 2003). Sodium is an especially important ion to monitor given that a decrease in the sodium concentration could be correlated with an increase in the instance of full body cramping (Baker, 2009). The concentrations of certain ions contained in sweat are given in Table 3, which also shows the changes in concentration before and after exercise. The data was obtained from sweat from the forearm of eight subjects, collected with a sweat patch comprised of gauze and parafilm (Morgan, 2004).

Ion	Hydrated State	Dehydrated State
Na+	81.1 mmol/L	91.1 mmol/L
Cl-	68.5 mmol/L	73.3 mmol/L

Table 3: Ion composition in sweat during and after exercise (Morgan, 2004)

Results collected from various physiological studies of sweat and ion composition note that the physiological range for sodium concentration in sweat is from 20mmol/L to 80mmol/L. This range can be prepared in lab by either mixing NaCl with water at concentrations within the given range, or diluting 1x DPBS as necessary. The calculation for determining how much NaCl involves determining the molecular mass of sodium and chloride and determining how much NaCl in grams is required to reach the desired concentration, as seen in Equation 1.

$$Na_{MolecularMass} = 23\frac{g}{mol}$$

$$Cl_{MolecularMass} = 35.453\frac{g}{mol}$$

$$NaCl_{MolecularMass} = 58.443\frac{g}{mol}$$

$$[NaCl] = \frac{20mmol}{L} => \frac{116.886mg}{100mL}\frac{NaCl}{H_2O}$$

$$[NaCl] = \frac{40mmol}{L} => \frac{223.772mg}{100mL}\frac{NaCl}{H_2O}$$

$$[NaCl] = \frac{60mmol}{L} => \frac{350.658mg}{100mL}\frac{NaCl}{H_2O}$$

$$[NaCl] = \frac{80mmol}{L} => \frac{467.544mg}{100mL}\frac{NaCl}{H_2O}$$

Equation 1: Weight (in milligrams) of NaCl needed per 100mL water to mimic sodium concentrations in sweat *[Where Na = Sodium; Cl = Chloride; H_2O = Water]*

1.3.2 Sweat Rates

The amount of sweat produced by the body is also an important indicator of sweat rate and overall dehydration. Every liter of water lost in the body during sweating corresponds to a loss of about 2.2 pounds in body weight (Coyle, 1994). If someone sweats at rate of one to two liters per hour, this means they could be losing between two and four pounds an hour (Coyle, 1994). This is a significant amount of weight loss that can lead to detrimental consequences if the fluids aren't replenished. Considering a 150-pound person, given the information in Table 1 at 4% loss of body weight to sweat this person is at risk of heat cramps – which corresponds to six pounds of overall fluid loss. Given weight loss corresponding to a sweat rate of 1.5 liters an hour, the six pounds could be lost in two hours. Without the ability to monitor this sweat rate in real-time, a 150-lb person could be at risk of debilitating cramps within two hours – whether it's a highly trained athlete, a soldier in the field of battle, or an elderly patient not being monitored closely.

1.4 RF Background

With the need for a sensing platform to non-invasively monitor hydration states defined, a suitable sensor emerged from initial studies performed with an RF resonator and low concentrations of the stress hormone cortisone. The response of the resonator to the liquid solution as opposed to air demonstrated the resonator's ability to detect the presence of liquid. After researching more about the electrical characteristics of the RF resonator, the reason for applicability in the sensing application became apparent.

1.4.1 What is an RF resonator?

An RF resonator is a combination of frequency-dependent, reactive components that exhibits a measureable frequency response. This system can best be explained by further modeling it as an electrical circuit, which is comprised of three components: a resistor (R), inductor (L), and capacitor (C), as seen in Figure 2.

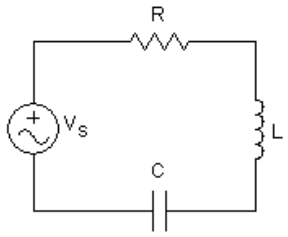

Figure 2: RLC circuit (Sinclair EET 155 site, 2011)

While the resistor is not a reactive element, both the inductor and capacitor are, meaning that they are frequency dependent components. The frequency dependent behavior is an important characteristic, because it's what provides a measureable signal that changes in the presence of different substances – like sweat. In electrical terms, this means that the impedance value of the resistor is constant across all frequencies, but the inductor and capacitor have impedance values that are dependent upon the frequency of the signal provided to the circuit. Similarly, if the value of the capacitor or inductor change, so will the frequency, and changes in the material in contact with the capacitor especially will alter the value of that capacitor. The relationships between frequency and corresponding inductive (L) and capacitive (C) values are given in Equation 2.

$$impedance_{resistor} = Z_R = R$$
$$impedance_{inductor} = Z_L = j\omega L$$
$$impedance_{capacitor} = Z_C = \frac{1}{j\omega C}$$
$$\omega = 2\pi f$$

Equation 2: Relationship between impedance and elements of RLC circuit (Robbins, 2000) *[Where ω=angular frequency; f = ordinary frequency]*

The RF spectrum ranges from 3 kHz to 300 GHz, with Table 4 showing the breakdown of the spectrum into commonly referenced terms. For the purposes of this project, only HF and UHF RF resonators were tested or fabricated.

Frequency	Abbreviation	Description
3-30 Hz	ELF	Extremely Low Frequency
30-300 Hz	SLF	Super Low Frequency
300-3000	ULF	Ultra Low Frequency

Hz		
3-30 kHz	VLF	Very Low Frequency
30-300 kHz	LF	Low Frequency
300 kHz – 3 MHz	MF	Medium Frequency
3-30 MHz	VHF	Very High Frequency
300 MHz – 3 GHz	UHF	Ultra High Frequency
3-30 GHz	SHF	Super High Frequency
30-300 GHz	EHF	Extremely High Frequency

Table 4: Frequency designations of Radio Frequency spectrum (Beasley, 2008)

1.4.2 Characteristics of RF Resonator Response

The combination of the components in the RF circuit determines the overall frequency behavior of the circuit and, as a consequence, its frequency response. Appropriate choice of R, L, and C are made so that the frequency response exhibits a resonance at a desired frequency. The RF resonator is essentially a notch filter that resonates at a frequency dictated by the values of capacitance and inductance chosen. Equation 3 denotes the relationship between the values of L and C and the resulting frequency.

$$f_R = \frac{1}{2\pi\sqrt{LC}}$$

$$C = \varepsilon\frac{A}{d}$$

$$\varepsilon = \varepsilon_r\varepsilon_o$$

$$\varepsilon_o = 8.85x10^{-12}\frac{F}{m}$$

Equation 3: Resonant frequency calculation, as well as capacitance calculations (Robbins, 2000) *[Where f_R= ordinary resonant frequency; L = Inductance; C = Capacitance; A = Area of capacitor plate; d = distance between capacitor plates; ε = permittivity; ε_r = relative permittivity; ε_o = vacuum permittivity]*

In addition, the parameters that contribute to the capacitance value are given in Equation 3. These equations demonstrate how the RF resonator is able to detect changes in both sweat volume and sweat composition. The capacitance value is affected by the dielectric (ε_r) of the material in contact with the capacitor. The difference between the dielectric constant of air and water is almost two fold, resulting in an increase in the capacitance of almost two fold. This in turn changes the resonant frequency of the RF resonator, and the changes can be correlated to the material in contact with the resonator. Changes in conductivity will also cause a change in the response of the resonator, weakening the measured signal as the conductivity of the material in contact with the resonator increases. In these ways, both sweat volume and sweat ion composition can be monitored by the RF resonator by capturing it's response in real-time as sweat builds up on the skin.

1.5 Measuring the RF Response

1.5.1 Parameters of RF Response

The effects of the changes in dielectric and conductivity on the response of the RF resonator can be seen in Figure 3, with the change represented by the darker, purple trace.

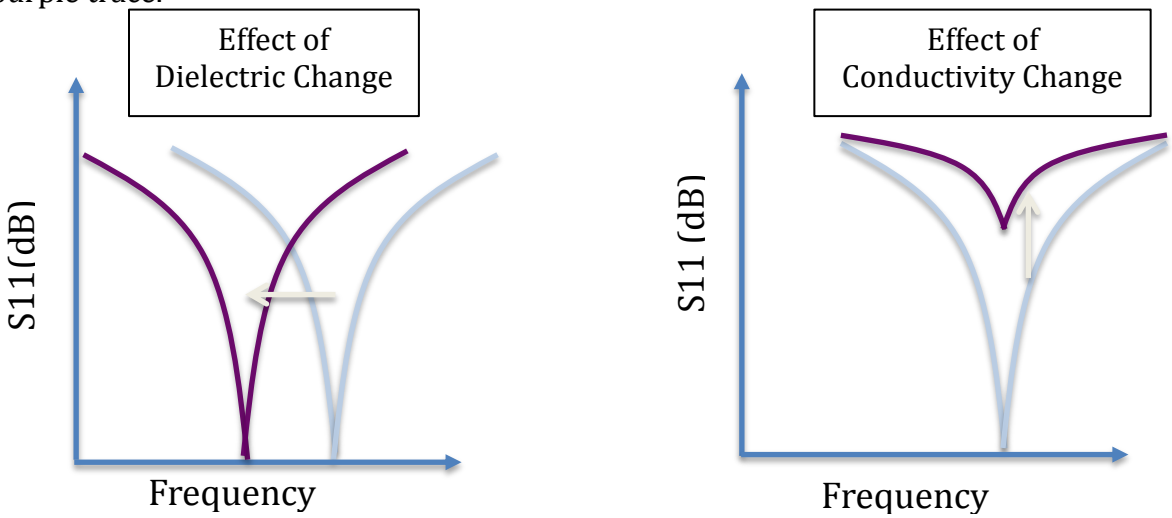

Figure 3: Effects of changes in dielectric and conductivity on response of RF resonator

In these representative plots, the parameters measured are frequency and the S11 parameter – which measures the reflected power. These are measured via S-parameters, and give valuable information about the behavior of the resonator. Another parameter that can be measured is the impedance of the resonator, because as Equation 2 evinces the impedance of the inductor and capacitor are frequency dependent. Therefore, any substance that causes a frequency shift will also bring about a change in overall impedance.

Another measure of the RF response is the Q, or quality, factor, which is defined as the ratio of the resonant frequency to the bandwidth of the signal. Normally, the bandwidth is determined to be the lower and upper frequency values at the 3dB S11 measured point because that is where 50% power loss is assumed – also known as the Full Width at Half Maximum (FWHM). However, in the measurements made for this project, the overall reflected power was sometimes not more than 3dB overall, so a different algorithm was developed to calculate the Q factor. Instead of measuring the bandwidth at 3dB, the overall reflected power at the minimum frequency was determined and half of that reflected power value was used as the point at which the bandwidth was measured.

1.5.2 S-Parameters: Transmission and Reflection

In order to measure the response of the RF resonator, a signal has to be transmitted to the resonator and the measured response is recorded. This is accomplished using a Vector Network Analyzer (VNA), and a primary powered antenna that is connected to the VNA. For a wireless coupling application, the

powered primary coil will induce a magnetic field in the secondary RF resonator that is being used as the sensing device. At the resonant condition, the measured reflected power will be lowest and represented by the characteristic spike seen in the frequency response in Figure 3.

The characterization of the electrical behavior of the network under test can be represented by a number of sets of parameters, the most relevant being: Y-parameters, Z-parameters, and S-parameters. Table 5 summarizes the similarities and differences of these three sets, and also highlights why S-parameters were utilized for this project.

Type	Parameter Measured	Measurement Condition	Benefit	Drawback
Y-Parameters	Admittance	Short Circuit	Relatively intuitive measurement to interpret	Noise in measurement & hard to measure at high frequencies
Z-Parameters	Impedance	Open Circuit	Relatively intuitive measurement to interpret	Noise in measurement & hard to measure at high frequencies
S-Parameters	Scattering	Matched loads	Easier to measure power at high frequencies	Relatively difficult measurement to interpret

Table 5: Comparison of parameters measured in linear electrical network (Heck, 2008)

With matched loads, the scattering parameters – or S-parameters – make it easier to take measurements at high frequencies, and are therefore the measurements by the VNA. Both Y and Z-parameter measurements present challenges at high frequencies, because open circuit capacitance and short circuit inductance have large contributions at high frequencies (Heck, 2008).

The VNA has two ports, and can make either one-port or two-port measurements. Both measurement types were made in this project, but the majority were one-port reflection measurements. One-port measurements are known as reflection measurements, while two-port measurements are called transmission measurements – given the path that the signal follows as it is either reflected within the port or transmitted from one port to another.

1.5.3 Logarithmic Magnitude Plot

Figure 3 demonstrates one of many possible charting options that the VNA offers. This type of chart is known as a logarithmic magnitude (log mag) plot, and displays the reflected power in decibels (dB) as a function of frequency. This gives

an indication of the resonant frequency, because at that point the reflected power is essentially zero as the impedance values of the capacitive and inductive elements cancel each other out. The output shown in Figure 4 is a direct screen capture from a VNA of a log mag plot.

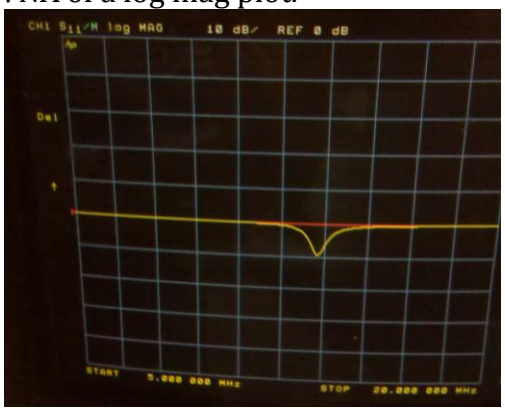

Figure 4: Log Mag plot captured from screen of HP8753D VNA

1.5.4 Smith Chart

In contrast to a Log Mag plot, a Smith Chart is another output format from the HP 8753D VNA that plots the change in impedance as a function of frequency, as seen in Figure 5.

Figure 5: Smith Chart output format on HP 8753D (Jefferies, 2011)

The Smith Chart provides RF engineers with ability to further determine the electrical behavior of transmission lines and matched circuits (Wikipedia, visited March 2012). As plotted on the complex reflection coefficient plane in two dimensions, the chart separates the real and imaginary contributions of the impedance. It also shows whether there is a more capacitive or inductive contribution, with data points residing in the top hemisphere of the circular chart corresponding to inductive values while the bottom hemisphere corresponds to capacitive values. The line bisecting the Smith chart is the point at which the imaginary impedance is zero and this is where the RF resonator's measurement will pass through at the resonant frequency.

1.6 RF Resonator Design Considerations

The RF resonator is designed with two main parameters, the inductance and the capacitance. These are the two components that determine the resonant

frequency, and choosing the right values is tantamount to designing the resonator at a specific frequency. The geometry of the resonator dictates the inductive value – the number of turns, the width of the trace, and the spacing between turns. The capacitive element is then added to ensure that the resonant frequency condition is met. A typical RFID resonator produced by TI is shown in Figure 6.

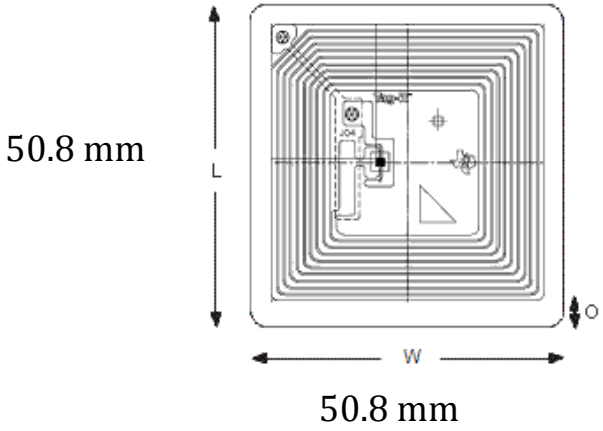

Figure 6: TI Tag-It RFID layout (TI, 2011)

Aside from the overall geometry and resonant frequency of the RF resonator, a number of other design parameters have to be considered – including the method of transmission and powering scheme.

1.6.1 Wireless vs. Wired Transmission

The electromagnetic properties of the RF resonator lend it to transmit a signal that can be received by another resonator that is tuned to the same resonant frequency – analogous to how transformers function (Robbins, 2000). When the primary resonator is powered by an AC source, the electric field produces a magnetic field. This magnetic field is then induced in the secondary resonator and in turn produces and electric field and current flow. The field lines of the magnetic field between the wirelessly coupled antennas are illustrated in Figure 7.

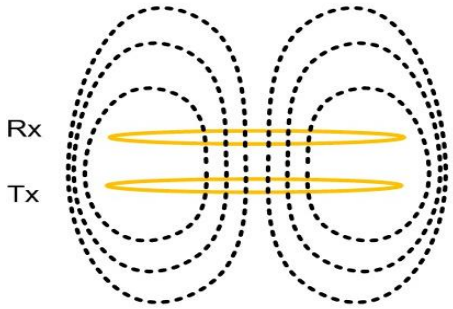

Figure 7: Inductive coupling model with two antennas (McIntosh, 2010)

This wireless powering and subsequent transmission of information about the behavior of the RF resonator was used as the basis for this project. While a wired setup was considered, the ability to utilize known wireless protocols for

communication and eliminate the need to be tethered to a device made the wireless setup the more desirable option.

1.6.2 ISM Bands

For wireless applications there are pre-determined frequency bands in which a device can operate. These bands are known as the Industrial, Science, and Medical (ISM) bands, which are reserved for RF applications and regulated accordingly (Wikipedia, 2011). As Table 6 illustrates, there are factors of each ISM band that make it more or less optimal as an operating frequency range for the RF resonator considered for this project.

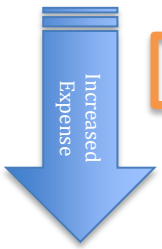

Min Freq.	Max Freq.	Center Freq.	Availability	Reading Range	Reading Speed
13.553 MHz	13.567 MHz	13.560 MHz		3-10 ft.	Medium
902.000 MHz	928.000 MHz	915.000 MHz	Region 2 only	10-30 ft.	Fast
2.400 GHz	2.500 GHz	2.450 GHz		10+ ft.	Fastest

13.56 MHz Devices are best for use in liquid/aqueous environment

Table 6: Key characteristics of ISM bands (Wikipedia, 2011)

While resonators in the 13.56MHz-centered band have beneficial characteristics such as being more suitable in liquid environments, they are also limited in their read range distances. In the higher frequency ISM bands, the read range gets much longer, but these resonators have poor performance near metals or water. For these reasons, the main frequency studied for this project was 13.56 MHz as it is best suited for an aqueous environment. At frequencies higher than 13.56 MHz, represented by the ISM bands centered at 915 MHz and 2.45 GHz, the energy absorption by water is too high (Avante website, visited March 2012). With the antenna's energy being absorbed by the surrounding aqueous environment, the coupling response is not effective enough to produce a measureable signal.

1.6.3 Read Range

Wirelessly coupled devices require a reader in order to receive information from the RF resonator. Depending upon the application, the distance between the RF resonator and the associated reader can be anywhere from a few inches to feet. This read range is based upon many parameters, including the size of the RF resonator and the size of the accompanying reader, as Figure 8 shows.

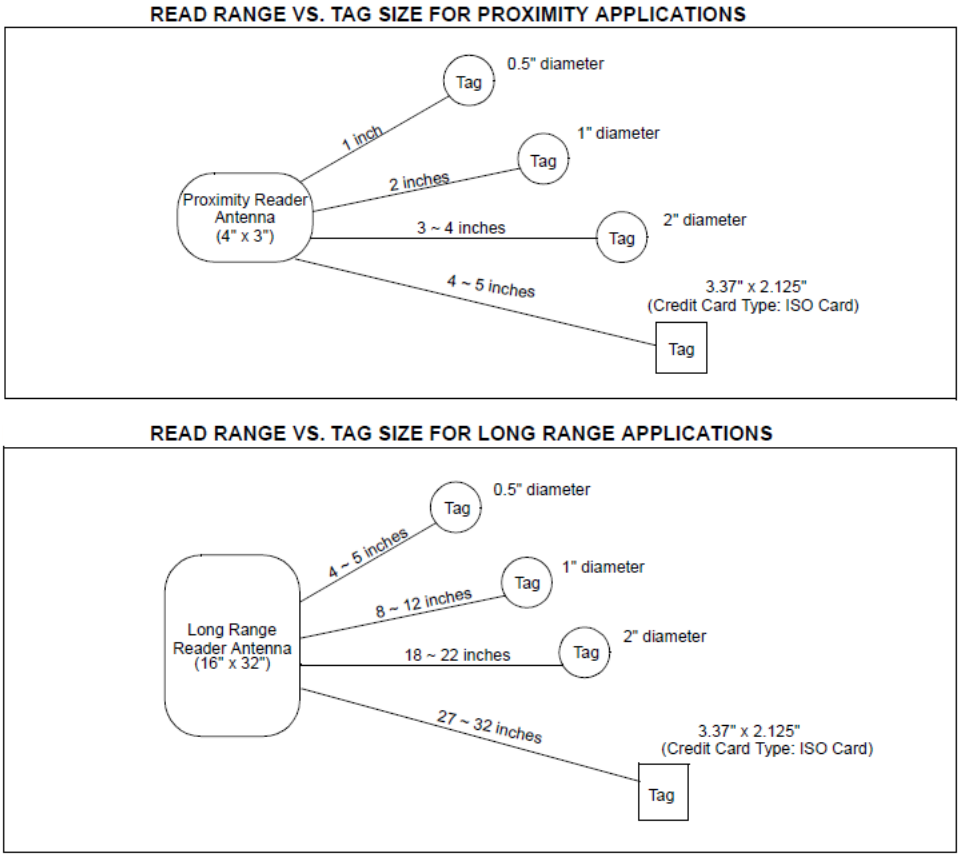

Figure 8: Associated read range for wireless RF application (Lee, 1998)

1.6.4 NFC vs. Bluetooth

Aside from the behavior of the resonators associated with the various ISM bands, another important factor is in the communication protocol utilized to transfer information wirelessly. Two major protocols on the market at the time of the publication of this thesis are Near Field Communications (NFC) and Bluetooth, outlined in Table 7.

	Bluetooth V2.1	BLE	NFC
RFID mode	Active	Active	ISO 18000-3
Standardization body	Bluetooth SIG	Bluetooth SIG	ISO/IEC
Network Standard	IEEE 802.15.1	IEEE 802.15.1	ISO 13157 etc.
Network Type	WPAN	WPAN	Point-to-point
Cryptography	Available	Available	Not with RFID
Range	~30m (class 2)	~50m	<0.2m
Frequency	2.4-2.5 GHz	2.4-2.5 GHz	13.56 MHz
Bit rate	1-3 Mbit/s	~200 kbit/s	424 kbit/s
Set-up time	< 6 s	< 3 ms	< 0.1 s
Power consumption	Varies with class	< 15 mA (xmit)	> 15 mA (read)

Table 7: Comparison of NFC and Bluetooth functionality (Montgomery, 2011)

Currently, only one mobile device on the market is equipped with NFC capabilities, the Samsung Galaxy Nexus. Before the advent of Bluetooth Low Energy (BLE), NFC was a more appealing option because it required lower power consumption. With BLE matching or even beating the power consumption of NFC, it becomes a tempting wireless protocol especially given the two-fold increase in read range over NFC. Utilizing either of these protocols would allow the RF sensing device to interface with mobile apps.

1.6.5 Active vs. Passive

While the operating frequency, coupling mechanism and material choices all play an important role in the design of the RF sensing device, they are not useful until they are provided with power. When designing an electrical device, power considerations are important as they can add cost - in terms of real estate on a circuit board and in material price. Table 8 outlines the differences between an active and passive device.

Passive Resonator	Active Resonator
Operate w/out battery	Powered w/internal battery
Less expensive	More expensive
Unlimited lifetime	Lifetime limited by battery
Lighter	Heavier due to battery
Subject to noise	Better noise immunity
Derive power passively	Internal power source from battery
Requires more powerful reader	Effective with less powerful reader
Lower data transmission rates	Higher data transmission rates

Table 8: Characteristics of Active and Passive Electrical Devices (UK RFID website, visited 2011)

Though an active device can operate without a reader and can act at higher data transmission rates, a passive device allows for the use of much fewer parts and a less complex design overall on the sensor side.

1.7 Prior Work

There was prior work performed that showed promise for the premise behind this thesis project. The experiments were conducted with RFID tags for liquid and gas sensing applications, as well as for monitoring sterile environments in liquid bioprocess manufacturing (Potyrailo, 2010). Figure 9 shows the results of an experiment performed to test the response of various salt solutions in the presence of RFID tags.

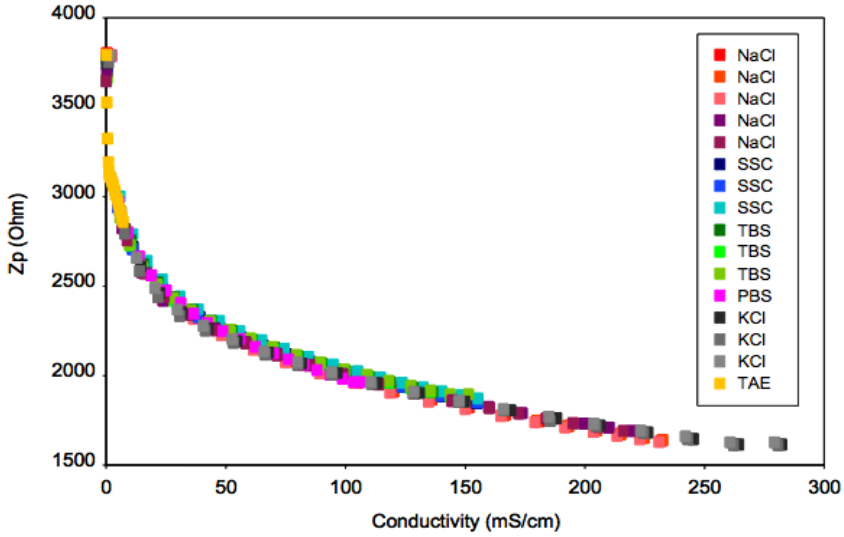

Figure 9: Relationship between conductivity of ionic solution and corresponding impedance measured by RFID tag (Potyrailo, 2010)

As the plot in Figure 9 shows, the response of the RFID tag is independent of the ion in the salt. The RFID tag is able to detect the difference in concentrations of salts, irrespective of the composition of the salt. For the physiological range of NaCl in sweat that is between 20mmol/L and 80mmol/L, the corresponding conductivity is between approximately 0 to 20 mS/cm. Given this promising start of existing research, the drive to start the task of developing a real-time, RF, non-invasive sensing device could begin in earnest.

2.Methods & Materials

2.1 Silk processing

As a biodegradable and biocompatible material, silkworm silk presented itself as an ideal candidate for an absorbing material in the development of a sweat patch prototype. Processed silk was further modified to create a silk sponge, capable of wicking solution and losing that same solution to evaporation – essentially cyclically hydrating and dehydrating.

The silk processing steps start with silkworm cocoons, which contain a deceased silk worm and have to be stripped of proteins that are not compatible with the human body. These cocoons are cut up to remove the silkworm and to help aid the process of boiling the material in a sodium carbonate water solution. This causes the silk to break down, and take on a more coagulated structure, which is removed from the boiling solution after 30 minutes and placed in a hood overnight to dry. The dried silk, which now looks and feels like cotton, is then mixed with lithium bromide solution to further process it for use in and on the body, and this mixture is placed in a 60 C oven for 3-4 hours until the silk is transformed into a viscous solution. This new form of silk is then transferred to dialysis cassettes using syringes, and the cassettes are placed in four-liter beakers of de-ionized water on a spinner plate in an effort to remove the lithium bromide. The water is changed six times over three days - three times the first day, twice the second day, and once the third day. At this point the silk is taken from the dialysis cassettes and placed in a falcon tube and centrifuged to remove excess particulate left over from cocoon or silkworm. The silk is then stored in a refrigerator and can be used for any number of applications. The process of purifying the silk from its cocoon beginnings to a biocompatible solution can be seen in Figure 10 below.

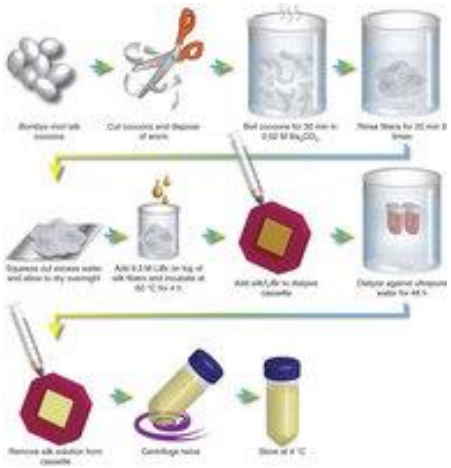

Figure 10: Silk processing steps (Rockwood, 2011)

2.1.1 Silk Sponges

The most relevant silk form factor for this project was a silk sponge. In order to produce a silk sponge, processed silk is placed in a petri dish lined with Teflon tape. The Teflon tape ensures that the silk sponge is easier to remove from the petri dish upon completion of silk sponge creation. 15mL of processed silk was poured into the petri dish, and then salt with a granule size of 600-700nm was evenly distributed over the area of the silk within the dish. The salt will dissolve and leave in its absence a space that acts as a pore that will allow the silk to absorb and evaporate liquid. Once the salt has been given enough time to dissolve, usually 2-3 days, the silk sponge is ready for use and is washed and removed from the petri dish, rolled up and stored in a falcon tube that is filled with de-ionized water.

2.2 Measurement Instruments

2.2.1 Network Analyzer

In order to measure the response of the RF resonator, a device is required to match the frequency of the resonator and interrogate the circuit. For the purposes of the experiments outlined in this project, a Vector Network Analyzer (VNA) was used. The VNA generally has two ports to allow for either transmission – a two-port measurement – or reflection – a one-port measurement. The majority of experiments conducted were taken as reflection measurements and therefore only utilized one-port of the VNA. The primary antenna attached to the port of the VNA is a loop antenna with an outer diameter of 1.5 inches on a printed circuit board (PCB). A BNC connector or SMA connector is attached to the PCB and this then connects to the VNA port via a 7mm-to-BNC connector or 7mm-to-BMC-to-SMA connector. When the RF resonator is placed in close proximity to the primary antenna - which is powered, - the electromagnetic coupling allows for measurements to be made over a pre-determined frequency range.

The first VNA used in these experiments was a HP 8753D. This device has a frequency range from 30kHz to 3GHz, and has a GPIB connection that can output results to a computer through a GPIB-to-USB adapter. A Matlab program, initiated by the user, was used to extract information from the VNA. The Matlab program worked either by extracting a one-time measurement when triggered, or was set up to extract measurements at pre-determined intervals over a given timeframe. This second measurement method was utilized for continuous measurements when dehydration studies were conducted. Dehydration experiments were conducted over timeframes often lasting multiple hours, and initially the dehydration profile of the material under test was unknown. Given that the Matlab program that extracted information from the VNA at pre-determined time intervals, it provided an ideal testing condition to generate the dehydration profile of a material in a methodical manner.

A second VNA was also utilized in later experiments, and was a homemade version constructed by Bob Melville - a ham radio and RF specialist (Melville, 2011). The reason for moving to another VNA was to explore the possibility of making measurements with a more portable device. The HP 8753D includes a monitor that

displays results and is a bench top device that measures in a frequency range from 30kHz to 3GHz, with a dynamic range of up to 110 dB (HP8753D Manual). The size and weight of the HP 8753D make it unwieldy for field applications in medicine or athletics, so a more portable option was explored. This portable VNA option was offered by Bob Melville and is his homemade VNA that he constructed in his lab, modeled after a VNA designed by Makarov (Makarov) as seen in Figure 11.

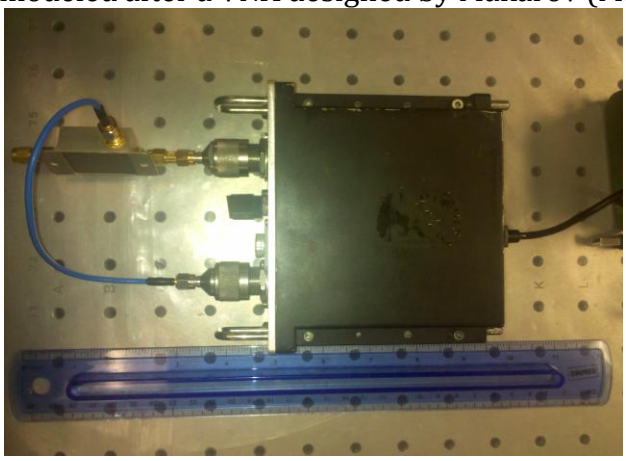

Figure 11: Portable VNA modeled after Makarov N2PK

Given that the dimensions of the enclosure that houses the VNA electronics shown in Figure 11 are 6.3"x6.3"x2.03", it's size makes the homemade VNA an ideal candidate for portable measurements in many environments – from the athletic fields to nursing homes. The connections used to attach the RF resonators to the Marakov-modeled VNA were 7mm-to-SMA, as the RF resonators chosen for experiments have SMA connectors.

Though there is no screen to display results, there is a USB connection to a computer and a companion computer program that works in concert with the Makarov-modeled VNA, known as myVNA. The myVNA program allows for different RF measurements to be taken and for storage of the results in a user-friendly interface. Though the Makarov-modeled VNA is portable, one drawback is that it works within a much smaller frequency range than the HP 8753D. As-is the Marakov-modeled VNA operates up to about 60 MHz, but an up-converter can be utilized that pushes the upper range of the measureable frequency to 500 MHz. This is beneficial for some of the RF resonators being tested, but means it can't be used for some UHF resonators that are in the 916 MHz and 2.4 GHz Industrial, Scientific, and Medical (ISM) RF bands.

2.2.2 Parameters Measured

A number of parameters were measured using both the HP8753D and portable VNA, in order to determine the change of the RF resonator in response to substances with different ionic concentrations or dielectric values. These included the frequency – in the MHz-GHz range depending on the design of the RF resonator, reflected power (dB), and impedance (ohms). These results were viewed in a variety of plots on the VNA depending on the information being plotted. Logarithmic

Magnitude plots displayed the S11 parameter (reflected) power as a function of frequency, while Smith charts showed the impedance as a function of frequency.

2.2.3 Mobile Device - Android

Another device used to detect the presence of a matched RF resonator was a Samsung Galaxy tablet. The premise of this detection device was different from the detection method employed by a VNA. While a VNA performs a frequency sweep and measured parameters over a given frequency range, the Android device was used to determine if an RF resonator at a specific frequency was present. An Android development kit used to interface with Android devices was used and was further modified. Additional hardware was designed and fabricated by others in lab to connect a PCB with a 13.56 MHz RF resonator to the Android development kit. A pre-existing Android software application known as the Basic Accessory Demo was then adapted to determine if an RF resonator matching the 13.56 MHz frequency of the primary resonator - attached to the Android development kit - was in range. Though the second, matched RF resonator had to be within a few centimeters of the primary 13.56 MHz resonator, the second resonator could be detected wirelessly given the modified app. A combination of Eclipse, which is a development tool for Java, an Android Software Development Kit (SDK) and an Android emulator were used to make the changes and additions to the Basic Accessory Demo app.

2.3 RF Resonators

2.3.1 Commercially available RFID tags

Initially, commercially available RFID tags were utilized for testing purposes, as seen in Figure 12, diagram 1. These commercially available RFID tags were TI Tag-It 13.56 MHz square resonators, consisting of aluminum trace, a chip capacitor, IC and substrate film to protect the reactive components (TI Tag-It, 2011). Though the IC is not something that is required for the implementation of a sensing sweat patch for this project, it was useful to start with the TI tags because they are readily available and cheap, costing about $1 each (Digikey, 2011). The TI RFID tag was placed on top of the primary ring antenna and readings were made with the HP 8753D VNA. Double-sided stick cellotape was used to affix the TI tag to the PCB with the ring antenna, as positional dependence plays a part in getting consistent RF measurements with the ring antenna and TI tag.

2.3.2 Fabricated RF Resonators

Once the TI tags proved effective, there was a need to incorporate RF resonators at different frequencies to determine the effectiveness of resonators within a variety of ISM frequency bands. Two considerations were taken into account when the new RF resonators were designed – a coplanar ring antenna and RF resonator implementation, as well as fabricating the resonators in house. With a coplanar ring antenna, the positional dependence of the two RF antennas required to make the measurement could be greatly minimized. The ability to fabricate the resonators in house afforded more flexibility in developing new RF resonators and shorter lead times in producing the new designs. The use of an LPKF milling

machine, model LPKF Protomat S103, made it possible to fabricate the new resonator patterns in the laboratory, on single-sided FR4 board with copper traces.

The first step in fabricating the resonators was to model the resonator trace in Sonnet. Sonnet allows the user to create the trace pattern and then run an electromagnetic simulation to determine the frequency response of the RF resonator trace. Before running the simulation certain parameters can be set to account for other elements that are not part of the RF trace, such as the parasitic capacitance value. Once the simulations in Sonnet provide results that align with the expected resonance, the geometry of the RF trace created in Sonnet is recreated as a 2D drawing in AutoCAD. This AutoCAD file is then importing into the software program that controls the LPKF milling machine and determines which drilling or milling bits to use to recreate the pattern. Once the AutoCAD file is loaded and the LPKF settings are adjusted accordingly, the pattern is etched out of the copper thereby creating the RF resonator at the desirable frequency. While the milled pattern ensured that the inductive element of the RF resonator was accurate, the resulting capacitance often wouldn't be adequate to produce the desired resonant frequency. In these cases, a capacitor was also soldered onto the milled pattern to achieve the appropriate resonant frequency. The resonant frequencies targeted corresponded to those found in four widely used ISM bands: 13.56 MHz, 433 MHz, 916 MHz, and 2.45 GHz.

One big design difference between the milled RF resonator and the TI Tag-It RFID resonator used in initial testing was the coplanar design. When testing the TI Tag-It resonator, a primary ring antenna was utilized that was physically separate from the TI Tag-It resonator. Instead, the new milled pattern included a coplanar design in which the loop antenna and RF resonator resided on the same PCB. This eliminated the need for ensuring fixed alignment when the two components were separate, as in initial testing with the TI Tag-It commercial RFID antenna. A ring antenna was designed to encompass the RF resonator pattern, and both were milled from the same piece of FR4 with copper trace. The connection to the VNA used for this coplanar RF resonator and loop antenna design milled in FR4 was an SMA adapter. This new coplanar design can be seen in Figure 12, diagram 2.

2.4 Sweat Patch Design

After the PCB fabricated RF resonators showed results indicating that these resonators could be used to detect changes in both water volume and ion concentration, the concept of a wearable sweat patch was explored. The end goal of the project was to create a wearable sensing device that would wirelessly transmit information about the state of hydration on the skin's surface. In order to design a sweat patch that could comfortably fit on the skin and conform to the skin's surface. Multiple design parameters were considered, including what material to use to ensure easy application on the skin, what material should be used to absorb the sweat, and how to create an RF resonator on a semi-flexible substrate. These materials are discussed in the sections below as components of a sweat patch sensor.

2.4.1 Absorbing Material

The first material investigated was an absorbing material intended to wick sweat from the skin's surface to bring it in contact with an RF resonator. Two general materials were tested for their efficacy based on literature searches and an analysis of materials currently used for sweat composition analysis. These two materials were woven-fiber cellulose as well as silk sponges. While both materials are biocompatible, the benefit of silk sponges is their ability to hydrate and dehydrate. With celluose patches, once they are saturated they cannot necessarily be reused as the composition of the material in compromised. However, silk sponges can absorb liquid and then be left to dehydrate, at which point they can again absorb liquid. The benefit of the cellulose is that it's a material already used in existing sweat patches that are sent to lab for analysis. Also, the cellulose is easier to obtain given that silk sponges can take up to two weeks to produce from the starting point of boiling the sink to the end stage of creating the sponges. Cellulose of varying thicknesses was tested from two manufacturers – GE and Pall. Dehydration studies were performed with both materials in order to quantify how well each performed in absorbing both DI water and concentrated salt-water solution.

2.4.2 Insulating Material

As testing progressed with liquid solution in contact with the RF resonator, the need for an insulating layer arose. This was mainly the case for ionic solutions, where an insulating layer proved valuable in reducing the overall attenuation of the signal. Without this layer the RF resonator was too sensitive to the solution and the signal was attenuated to a degree wherein differences in the response of the RF resonator to varying ionic solutions weren't easy to glean. However, with the introduction of an insulating layer the effect on the RF resonator was strong enough to still change the behavior of the resonator without dampening the signal too much.

Initially, materials that were readily available in lab were used for this insulating layer, such as parafilm. However, this material provided too much protection for the RF resonator and the signal was not within the desired detectable range. By expanding the search for thinner materials, two options emerged and were used for subsequent testing. The first option used for most of the initial testing with the bench top VNA was saran wrap, a material also used earlier studies found in the literature (Potyrailo, 2012).

While this was adequate for bench top testing, the drawback of using saran wrap in a sweat patch prototype is that it's not breathable. Using a non-breathable material could create a non-native microclimate of sweating on the skin's surface, which could skew measurements. For the sweat patch prototype, a more porous and breathable substance was required, which came in the form of tegaderm. The 3M tegaderm used for the sweat patches are commonly used for wound dressing applications given that tegaderm is designed to allow for breathability in only one direction. Uni-directional breathability ensures that wounds can breathe to foster healing, but protects the wound from outside environmental influences that could slow the healing process. Exploiting this property of tegaderm would allow appropriate movement of sweat and it's analytes to the RF resonator to detect changes in hydration at the skin's surface.

2.4.3 Shadow Masked RF Resonators

Tegaderm also proved effective as a layer on which to shadow mask a gold RF resonator pattern. The need to shadow mask a pattern arose as the PCB RF resonator designs were ported to a more comfortable form factor. Once the absorbing and insulating materials were chosen, the final important design constraint to overcome was in choosing the appropriate material to act as an RF antenna. While the PCB RF antenna produced in lab was able to detect changes in water volume and ion concentration, the PCB was not an ideal material for use on the skin's surface given its rigidity. Ideally, this would be accomplished by depositing a conductive material in an RF resonator design on a more conformal material than PCB.

The conductive material arrived upon was gold because it can be sputter coated to a desirable trace thickness on a variety of materials. In order to perform the sputter coating process, the NanoMaster Inc NSC-3000 tool was employed, with a gold target. Settings for sputter coating included a base pressure of 0.08 milliTorr, a sputter pressure to target of 5 milliTorr, and a DC power to gold target of 141 Watts. A shadow masking technique was used to transfer the RF resonator design to the target material. First, an adhesive sticker with the desired RF resonator design exposed is placed on the target material, with the adhesive covering all parts of the target material that do not contain any part of the RF resonator design. This combination of target material and adhesive sticker with the RF design exposed is then placed in the sputter coating tool, and a layer of gold is deposited on the exposed surface. For the purposes of the sweat patch prototype, the deposition layer of gold was tested at both 150nm and 300nm thicknesses. After the sputter coating process is complete, the sticker is removed from the target material, and a functional RF resonator is left behind.

The final target material used during the shadow masking was tegaderm, and this was the material used in the sweat patch prototype. Initially, saran wrap was used, and while this material was very easy to transfer adhesive stickers to and shadow mask gold patterns onto, it was not adequate for use with the final sweat patch prototype design. Attempts were made to shadow mask the gold RF resonator pattern onto cellulose, but this did not prove successful given the porous nature of the cellulose. The gold layer would not deposit evenly onto the cellulose surface due to absorption of the gold by the porous cellulose material. This rendered the RF resonator non-functional, given that an unbroken trace is required to transmit information at a desired and designed frequency.

Tegaderm proved to be the most successful and relevant target material, and a functional RF resonator was created on the surface of the tegaderm. An important fabrication tip in this shadow masking process is to weaken the adhesive strength of the sticker prior to placing it on the target material. If the adhesive is too strong in some cases the sticker cannot be removed without comprising the integrity of the sputtered RF resonator, including stretching of the pattern and even breakages in the trace. This was avoided by first weakening the adhesive strength of the sticker by repeatedly applying and removing the sticker from a surface. Once this step was performed, the sticker would still stick to the target material but would also be much easier to remove from the target material once the shadow mask process was

complete. An example of this shadow masked gold RF resonator pattern on a piece of tegaderm that has then been adhered to cellulose can be seen in Figure 12.3.

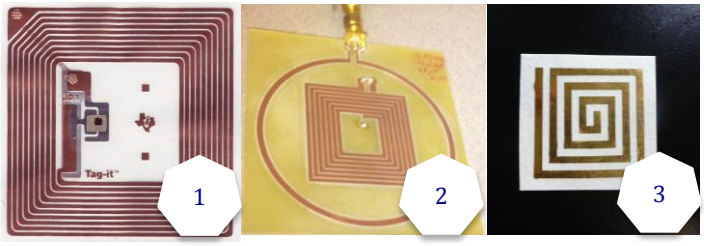

Figure 12: Progression of RF antennas – (1) TI Tag-It RF Transponder; (2) Milled co-planar RF antenna; (3) RF antenna Au-sputter coating on tegaderm & mounted on cellulose

2.4.4 Sweat Patch Prototype

The final sweat patch prototype was comprised of three main elements – cellulose, tegaderm, and a gold sputter coated layer of an RF resonator design. To assemble the patch, the RF resonator design is first deposited on the non-adhesive side of the tegaderm sample using the shadow mask technique. The functional RF resonator tegaderm sample is then adhered to a section of cellulose. At this stage, the sweat patch prototype has been assembled and can be placed on the surface of the skin. Once the appropriate placement on the skin is determined, a second piece of tegaderm - without any shadow mask pattern – is placed over the sweat patch prototype, both to keep the prototype in place and to protect it from the outside environment.

2.4.5 Sweat Simulator

In order to emulate the physiological response of sweating in the lab, a setup was constructed that fed the output of a syringe pump to a porous surface. The porous surface consisted of an acrylic layer with holes drilled to simulate pores in the skin through which sweat escapes. Acrylic was chosen because it is not a highly conductive material and therefore wouldn't interfere with the electromagnetic fields generated by the RF resonator. The tips of the syringe needles are placed in the holes and glued in place to keep them from moving. Tubing then branches using Y-connectors from the syringe pump and up through the needle tips to the surface of the acrylic. For the testing performed for this project, nine syringe tips were used and the holes in the acrylic were 0.024 inches in diameter. The syringe needles used were 22 gauge blunt-tip needles, and the tubing was clear and had an inner diameter of $1/16^{th}$ inch. All connections between the syringe, syringe tips and tubing were made using luer lock fittings.

The rate of fluid dispensed is controlled by the syringe pump flow rate and can be adjusted to mimic sweat rates that are physiologically relevant in humans. The syringe pump used was the NE-1000 from syringpumps.com, and can dispense fluid at either a given flow rate – ul/hr, ul/min, ml/hr or ml/min – or for a specified

volume. Both the syringe pump and the setup built to perform as a sweat simulator in lab can be seen in Figure 13.

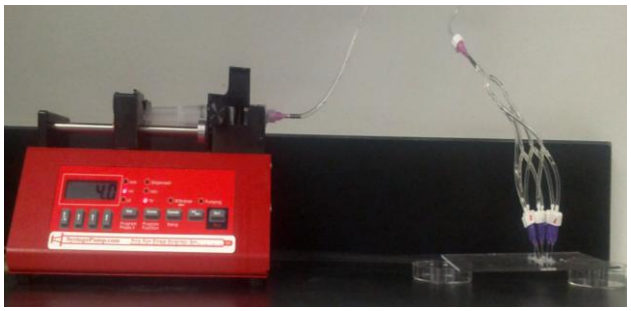

(1)

(2)

(3)

Figure 13: (1) Complete sweat simulator setup; (2) close-up of syringe pump, showing adjustable settings; (3) close-up of syringe needles leading to "pores" in acrylic

2.5 Performance Analysis

A variety of experiments were conducted, from proof of concept tests to ensure that changes in ion concentrations could be detected with an RF resonator to sweat patch prototypes testing. These tests are outlined in the sections below, in the order that they were conducted as the project progressed.

2.5.1 Analytes Tested

Initially de-ionized (DI) water was used in testing, to ensure that the approximately two-fold difference in the dielectric between air and water translated to a change in the response of the RF resonator. Once this change in response was noted, saline solution at different concentrations was tested to determine if the change in ionic concentration could also be correlated to changes in the electrical response of the RF resonator. At first, varying concentrations of NaCl were used, knowing that the physiologically relevant range of sodium in sweat is 20-80 mmol/L. Additionally, 1x Dulbecco's Phosphate-Buffered Saline (DPBS) solution was used to perform the same set of tests, because DPBS contains most of the other

components in human sweat, including potassium and magnesium. Given that the concentration of NaCl in 1x DPBS is about 140mmol/L, the DPBS was diluted to put the concentration of NaCl in the range of 20-80 mmol/L.

Aside from the DI water, NaCl, and DPBS solutions used for analyte and volume detection testing, two other materials were used in another set of tests. Silk sponges and beef tenderloin cutlets were used in dehydration studies, to determine the RF response of the resonators as a material in contact with resonator lost and gained fluid. Beef tenderloin was used as it an analog for dehydration at the skin's surface. Roast beef slices were also used to test the penetration depth of the signal emanating from the RF resonator.

2.5.2 Analyte Detection Experiments

The first set of tests was in place to determine the sensitivity of the RF resonator to changes in ionic concentration. DI water, NaCl and DPBS solutions were placed in contact with the RF resonator and the corresponding response was measured using a VNA. An insulating layer was required to ensure that the signal wasn't diminished so much that there was no easily measured response. Saran wrap was used as an insulating layer, and was affixed to a rigid surface in order to enclose the liquid under test. The best method utilized to create a well-sealed enclosure was to adhere the saran wrap to a piece of acrylic using double-sided cellotape. The acrylic in turn had a circle cut out in which the liquid was poured. The cut out held up to 5mL of solution, and the acrylic was a preferable material because it isn't conductive and wouldn't interfere with the electromagnetic properties of the RF resonator.

2.5.3 Volume Detection Experiments

As important as the analyte detection was the ability of the RF resonator to detect the build-up of sweat. This scenario was accounted for in volume detection experiments. Instead of putting the 5mL of solution in contact with the RF resonator at once, the solution would be distributed in smaller quantities and response of the resonator was measured as the volume of solution increased. This created a set of experiments that emulated the build-up and subsequent loss of sweat on the skin's surface as dehydration occurs.

2.5.4 Signal Strength Experiments

Given that the measurements made are wireless, the detection range between the two RF resonators was important to measure. A separation between the primary ring antenna and the RF antenna was introduced over increasing intervals, and the signal strength as a function of reflected power (dB) was measured using the VNA. The separation was created by placing numbered pieces of paper, up to 32 pieces, between the two antennas. Paper was used because it's not conductive and wouldn't interfere with the measurement.

As well as the signal strength between the two resonators, the penetration depth of the RF signal in tissue was measured. It was important to ensure that the presence of tissue wouldn't alter the signal in such a way that it was no longer

measureable. This was accomplished by placing slices of roast beef – one slice at a time – on top of the RF resonator and measuring the response on the VNA.

2.5.5 Dehydration Experiments

In preparation for testing with the sweat simulator and with human subjects, the ability of the RF resonator to detect changes in hydration states in real-time was tested. Initially, a piece of beef tenderloin was placed on top of the RF resonator and allowed to dry out over a time period of between three and eight hours. As the beef dehydrated, the response of the RF resonator was measured using the VNA. The same test was done using silk sponges, to ensure that the RF resonator could detect changes in dehydration whether it was in direct contact with the skin or with an absorbing material that was wicking sweat from the skin's surface.

In addition to the changes in the RF resonator, changes in the weight of both the beef and silk sponge samples were recorded. This allowed for the correlation of amount of fluid lost to changes in the RF response of the resonator. Two samples of beef or silk sponges that were similar in size and weight were used. One sample was placed on the resonator and RF parameters were recorded. The second sample was placed on a scale in the same lab as the first sample, and the weight was recorded over time. Any weight change was attributed to loss of fluid.

2.5.6 Sweat Collection Experiments

Before sweat was collected from human subjects, the RF response of the resonator to a constant flow of solution was tested using the sweat simulator. DI water was presented to the resonator by adjusting the flow rate of the syringe pump and the corresponding response was measured using the VNA. Once this set of tests proved promising, sweat patches were placed on human subjects.

The sweat patches tested on human subjects were cellulose only, and didn't include the gold RF resonator sputter coated onto tegaderm. In these human tests, a cellulose patch was weighed and the response of the RF coil to the patch was measured before exercise. The patch was then affixed to the lower back of the subject using medical grade tape, and the subject was asked to exercise vigorously in an indoor gym for 30 minutes. At the conclusion of the exercise, the cellulose patch was removed from the subject, weighed and then placed on the RF resonator and the response was measured using the VNA.

3.Results

3.1 Volume Detection Experiments

The effect of increasing volume of solution in contact with the RF resonator was tested, in an effort to determine if the resonator could detect a condition similar to sweat build-up on the skin's surface. Figures 14.1 and 14.2 below show how the frequency of the RF resonator shifted lower as 1X DPBS solution was deposited onto the RF resonator in increments of 0.5mL.

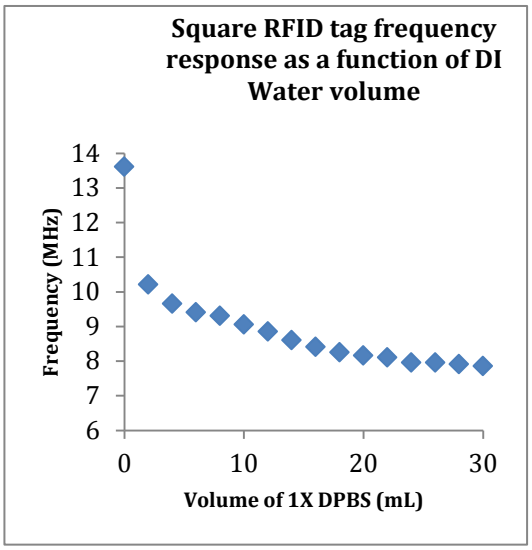

(1)

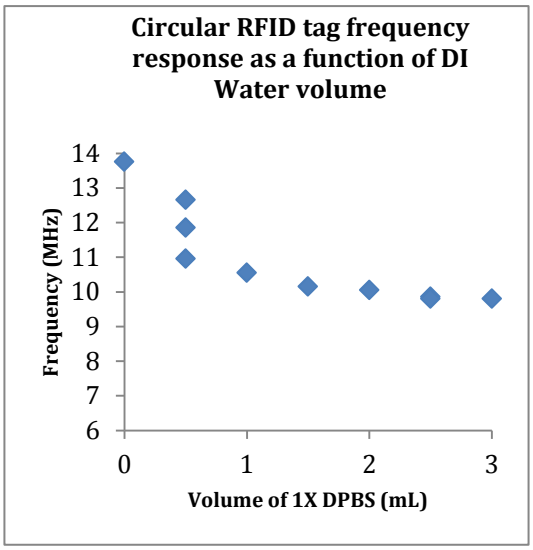

(2)

Figure 14.1 & 14.2: Effect of increasing volume of DI water in contact with TI Tag-It RFID tag, both square and circular geometries

Both a square and circular geometry of the TI Tag-It RFID resonators were tested, with the square geometry performing better. The decision was made to proceed with the square TI Tag-It resonator geometry for all future testing. As more DI water was added, the frequency shifted lower, showing that there is a correlation between amount of sweat and frequency response of the RF resonator.

3.2 Analyte Detection Experiments

3.2.1 Reflection Measurements

Initial experiments were conducted to determine if RF resonators would have unique responses to physiologically relevant concentrations of ions in solution. These were performed as reflection measurements on the HP753D VNA. Given that sodium is the most prevalent ion in sweat (Maughan, 1996), solutions of NaCl were prepared to test the frequency response of the RF resonators when put in contact with the NaCl solution. The physiologically relevant range of sodium in sweat is between 20mmol/L and 80 mmol/L, and so the upper end of the range and an intermediate concentration were chosen for initial testing – namely, 80 mmol/L and 40 mmol/L. DI Water was also tested to ensure that there was a discernible difference in the frequency response of the resonator to de-ionized and ionized solution.

The first RF resonator tested was the TI Tag-It RFID, and the results can be seen in Figures 15.1 and 15.2. For the first iterations of testing, both the minimum frequency and center frequency were measured, as the solution was deposited on the RF resonator one milliliter at a time. A layer of saran wrap was placed between the resonator and the solution as a layer of insulation.

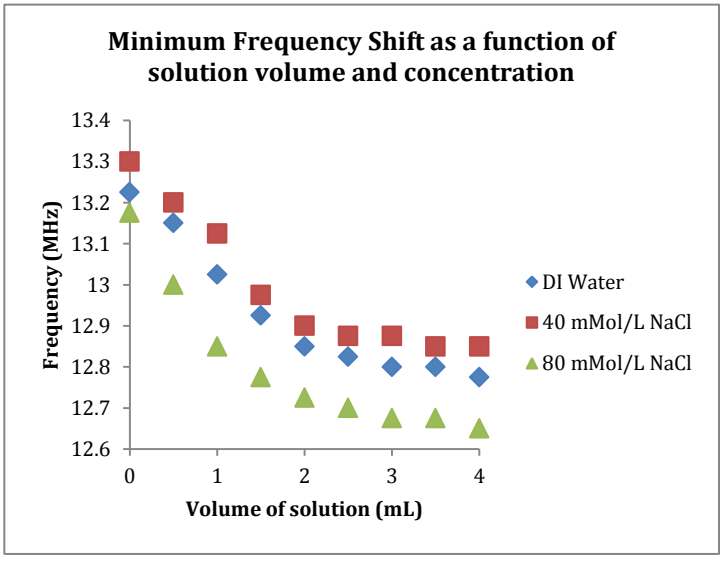

(1)

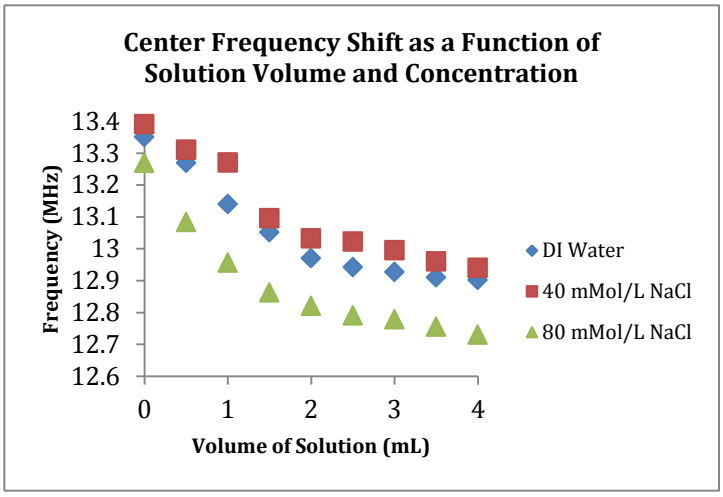

(2)

Figures 15.1 & 15.2: Shift in resonant frequency, both minimum (1) and center (2), of the TI Tag-It RFID as a result of deposition of different concentrations of NaCl solution

These results indicated two promising trends – one related to detection of different ionic solutions and the second related to overall sweat rate monitoring. There was a detectable difference in the frequency shift associated with 40 mmol/L and 80 mmol/L solutions, with the higher solution causing a greater frequency shift. Additionally, the frequency shift was also dependent upon the amount of solution present. This last trend was echoed in initial testing performed with 1X DPBS solution and added more credence to the ability of the RF resonator to act as a sweat volume detector.

With these initial results completed, further testing was performed to determine the sensitivity of the TI Tag-It RFID resonator to varying concentrations of NaCl solution. A number of solutions from 0 mmol/L (DI Water) up to 145 mmol/L were prepared and tested, with the complete list of NaCl concentrations tested given in Table 9. The decision was made to test concentrations of NaCl well outside the documented physiological range of sodium measured in sweat, to further test the limits of detection of the RF resonator.

Saline NaCl Solutions Tested (mmol/L)
7.86
15.74
23.61
31.48
39.34
60
80
100
120
145

Table 9: NaCl concentrations tested on TI Tag-It RFID resonator

In these rounds of tests, an additional parameter of the RF resonator was measured – the Q factor. While the frequency of the RF resonator is an important parameter to measure, the Q factor also provides useful information about the overall strength of the response of the resonator. 10mL of solution was placed in a modified falcon tube, with the bottom cut off to expose both ends, and one end of the tube covered in saran wrap to provide a thin insulating barrier between the solution and the RF resonator. The results of this set of experiments can be seen in Figure 16.1 and Figure 17, and the falcon tube enclosure can be seen in Figure 16.2.

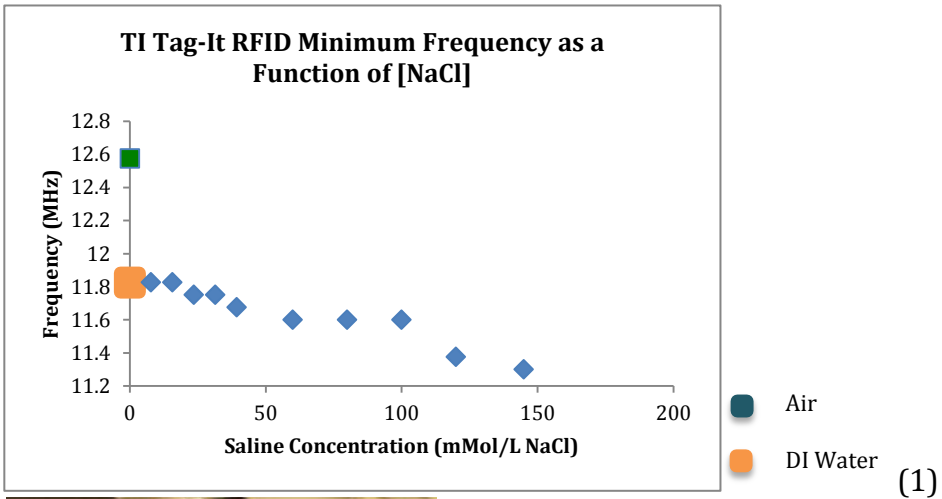

(1)

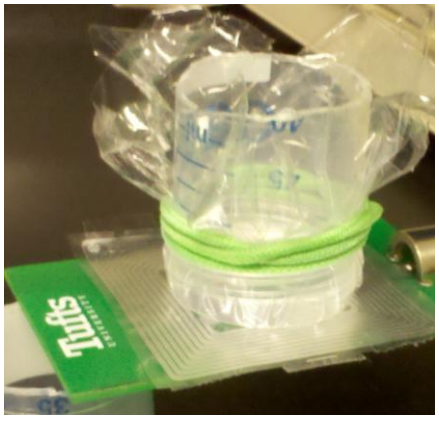

(2)

Figure 16.1 & 16.2: (1)Frequency response of TI Tag-It RFID to varying concentrations of NaCl solution; (2) Initial setup used to encapsulate saline solution in protective layer in contact with TI Tag-It RFID

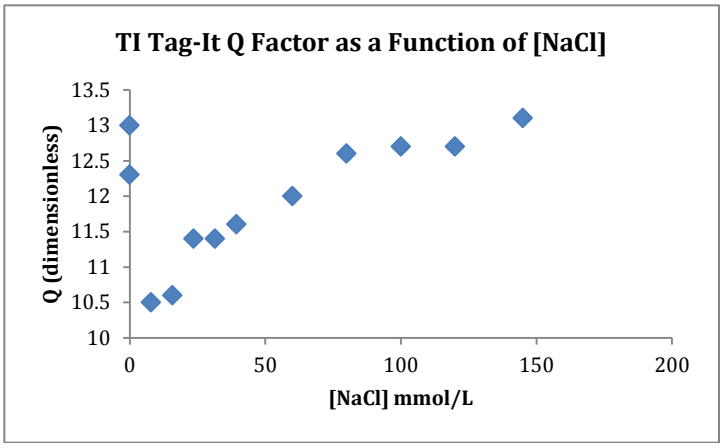

Figure 17: Change in Q factor in response to varying solutions of NaCl in the presence of a TI Tag-It RFID

The frequency shift of the TI Tag-It RFID resonator was correlated to the change in NaCl concentration, as the concentration increased so did the frequency shift. On the other hand, the relationship between Q factor and NaCl concentration seemed less straightforward. Initially the Q factor declines, but then climbs back to the original value.

Further testing of the correlation between frequency shift and NaCl concentration was performed over three consecutive days, and the results can be seen in Figure 18. The results showed that even though the conditions in the lab might have been slightly different from day to day, the overall trend of a decrease in frequency in response to an increase in NaCl concentration remained.

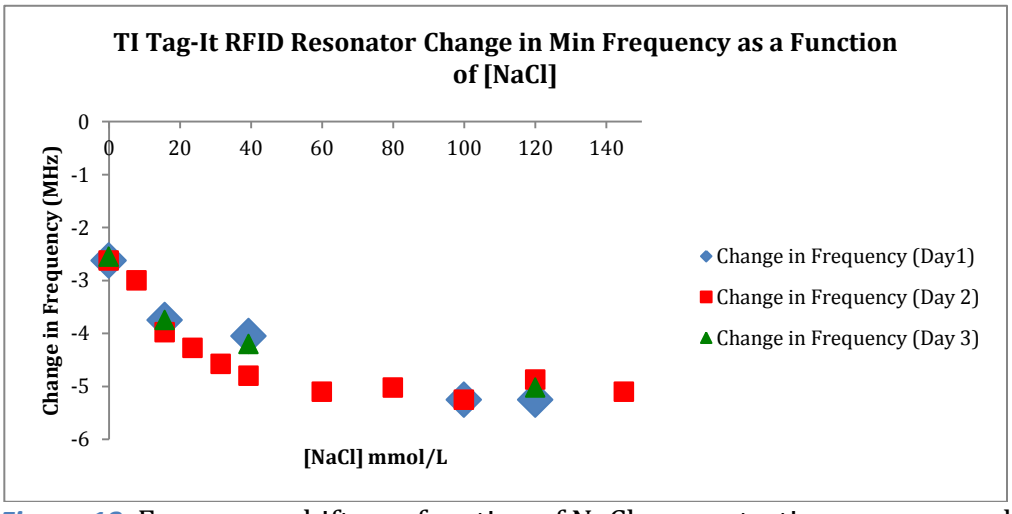

Figure 18: Frequency shift as a function of NaCl concentration as measured over three days for a TI Tag-It RFID

3.2.2 Transmission Measurements

An additional set of transmission measurements was made as a validation of the results gathered with the reflection measurements. Aside from being a transmission measurement, there were two other major differences between this

set of results and the reflection data sets. One was that the RF resonator used was a fabricated resonator built by Bob Melville to emulate the 13.56 MHz resonant frequency of the TI Tag-It RFID. This was a geometric design that had an inductance of 22 uH, with a 56 pF capacitor soldered on the fabricated RF resonator to bring the resonant frequency to 13.56 MHz. Four NaCl concentrations were tested – 20, 40, 60, and 80 mmol/L – and the results of the measured Q factor can be seen in Figure 19.

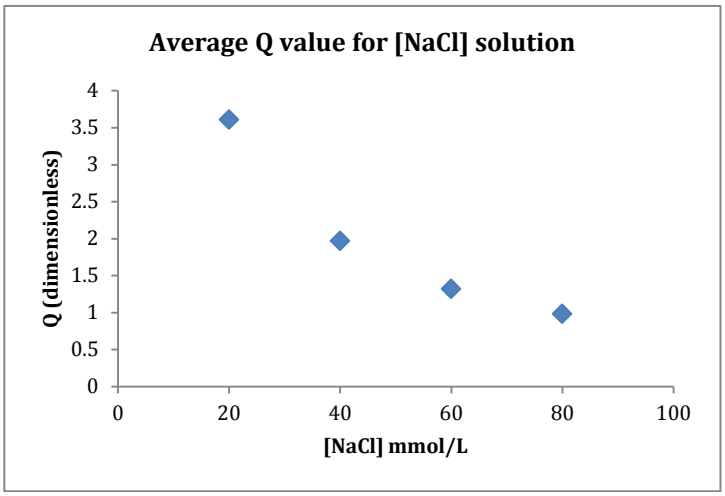

Figure 19: Measured Q value for various NaCl concentrations taken using transmission setup

The second difference in the set of measurements made in transmission mode was that the power provided to the RF resonator was direct and not provided through coupling with a primary coil. This meant that the leads coming from the HP 8753D VNA were connected directly to SMA connectors on the RF resonator. This was a design decision made by Bob Melville, in order to remove any perceived interference in the results previously obtained through wireless reflection measurements. As Figure 19 reveals, there is a correlation between Q factor and NaCl concentration, given that the Q factor diminishes in the presence of increasing NaCl solution concentration.

3.3 Signal Strength Experiments

As experiments continued, it was apparent that proper alignment between the primary loop and antenna and secondary RF resonator was integral to obtain positive results. These findings were bolstered by background research on electromagnetic coupling of resonators. In an effort to quantify this alignment, experiments were conducted both to test the optimal spacing between the primary and secondary resonators, as well as the most favorable positioning of the independent secondary resonator in relation the fixed primary resonator.

3.3.1 Positional Dependence

Liquid that came in contact with RF resonator through the course of the experiments was not uniformly distributed over the surface of the resonator. Therefore, a series of experiments were conducted to determine the response of the

RF resonator to solution deposited in a variety of locations on the resonator. Figure 20 illustrates where on the resonator 20uL of 1x DPBS was placed, and Table 10 shows the corresponding response of the resonator. In addition to frequency, the resistance, reactance, and inductance were also measured in an effort to provide a complete electrical response.

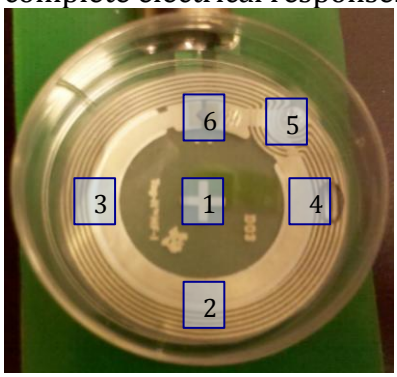

Figure 20: Six locations on TI Tag-It RFID where 20uL of 1x DPBS was deposited

Position on coil	Frequency (MHz)	Resistance (ohm)	Reactance (ohm)	Inductance
N/A (Air)	13.8	113	26	296nH
1	13.8	113	26	296nH
2	13.2	233	327	4uH
3	13.4	210	95	1uH
4	13.25	93	23	273nH
5	N/A	180	312	4uH
6 (chip)	N/A	-57	504	6uH

Table 10: Response of TI Tag-It RFID to 20uL of 1x DPBS deposited at six different locations on the resonator

While the middle of the resonator didn't show any change in response to the presence of 1X DPBS solution, all other areas of the RF resonator showed a marked change.

A further consideration in ensuring accurate measurements was alignment of the primary ring antenna and secondary RF resonator. The assumption was that the optimal placement was with the RF resonator positioned over the center of the primary ring antenna. This assertion was reinforced by the results shown in Table 11. The frequency and reflected power provided the most important results, with the impedance also measured to provide additional information if necessary.

Position of RFID tag	Frequency (MHz)	S11 (dB)	Impedance (ohms)
Centered	13.625	-34.1	52
Ahead	13.625	-14.3	119
Right	13.775	-2.4	391
Left	13.775	-2.5	276

Table 11: Effect of position of independent RF resonator with respect to fixed primary loop antenna on strength of RF signal

When the RF resonator was moved around in varying orientations, the coupling between the two resonators changed. The strongest coupling was shown to be in the centered alignment, as given by the largest absolute value of the S11 measured value – analogous to the reflected power – in Table 11 for this alignment.

3.3.2 Read Distance Testing

While the positioning and alignment of the two resonators is important, so is the distance between the resonators. For most of the testing the wireless connection between the two consisted of a minimal distance. The RF resonator was placed on top of the primary ring antenna, with a thin spacing of air that provided separation. In order to measure the effect of increased separation, pieces of paper cut to size to cover the RF resonator were placed in between the primary loop antenna and the 13.56 MHz TI Tag-It RFID resonator. As each piece of paper, measuring about 0.12mm in thickness, was placed a reading was taken of the measured S11 (dB) value and the results can be seen in Figure 21.

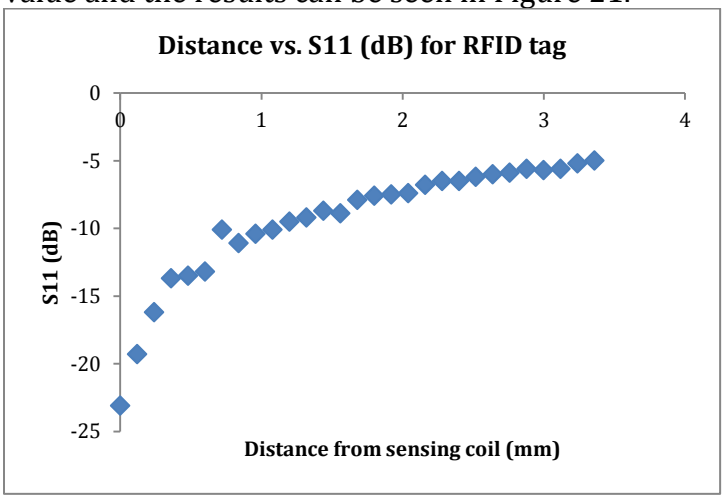

Figure 21: Effect of increased spacing on measure reflected power of a TI Tag-It RFID resonator

The spacing between the coupled resonators has a dramatic effect on the overall measureable signal strength. Once a minute distance of 2mm has been introduced, the signal strength has decreased five-fold.

3.3.3 Roast Beef slice experiments

After the strength of the coupling was measured, another interesting testing scenario arose. It was unknown how the RF resonator would perform in the presence of tissue, such as the skin, so a set of experiments was executed to determine the response of an RF resonator to surrounding tissue.

Roast beef slices were chosen as a tissue sample, and were stacked one slice at a time on the RF resonator, with a layer of saran wrap between the resonator and the roast beef to act as insulation for the signal. The experiments were carried out

on both the TI Tag-It RFID and the RF resonator fabricated in lab on FR4 with copper traces, both with a resonant frequency of close to 13.56 MHz. The frequency and S11 parameters were recorded as each slice of roast beef was stacked on. The results of the experiment on the TI Tag-It RFID can be seen in Figures 22.1 and 22.2, and the results for the fabricated RF resonator can be seen in Figures 22.3 and 22.4.

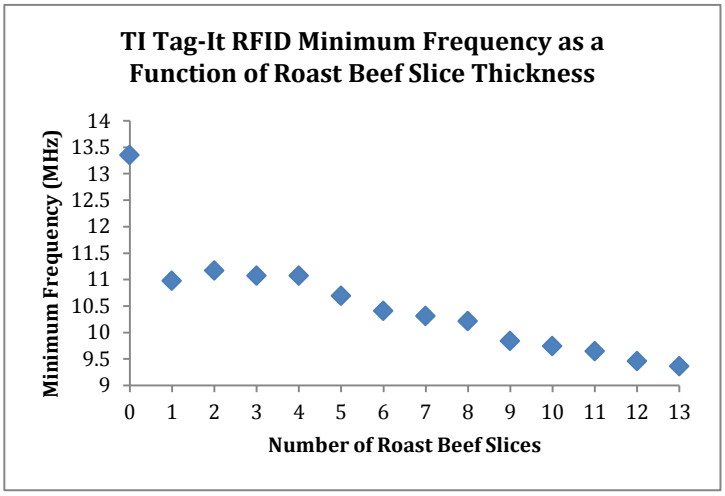

(1)

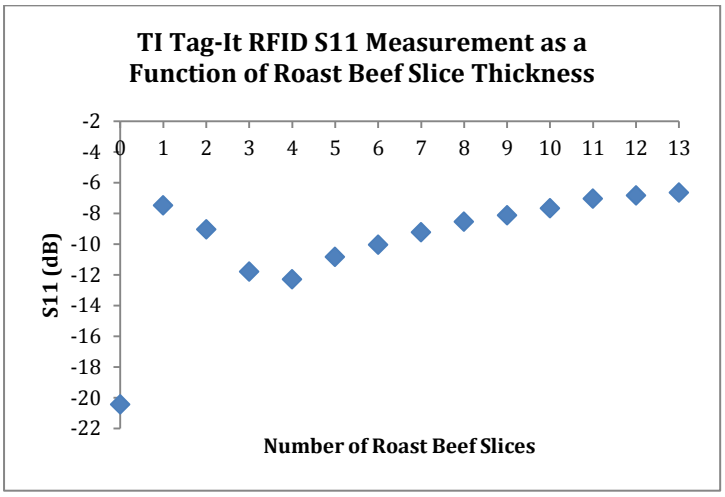

(2)

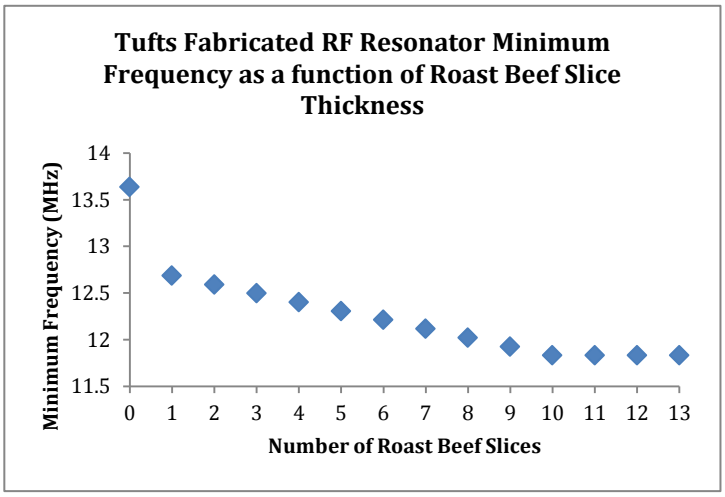

(3)

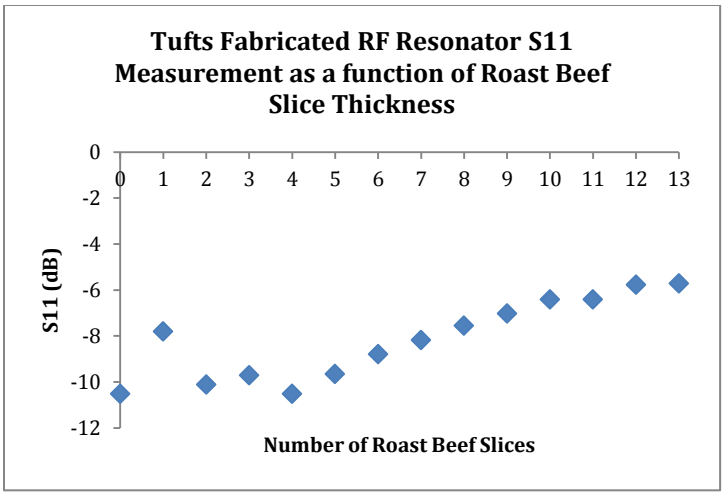

(4)

Figures 22.1, 22.2, 22.3, & 22.4: The effects of stacked roast beef slices on the frequency (1) and S11 parameter (2) of the TI Tag-It RFID and the frequency (3) and S11 parameter (4) of the fabricated RF resonator

For both the commercial TI Tag-It RFID and the fabricated RF resonator, there was a definite correlation between the frequency and the penetration depth of the tissue. The frequency decreased with the introduction of more roast beef slices and a greater overall penetration depth. The correlation between reflected power and penetration depth wasn't as clear-cut, with an initial decrease in the measured reflected power followed by a gradual increase.

3.4 Dehydration Experiments

With positional dependence and coupling separation characterized, a series of dehydration experiments took place. Already established was the ability of the RF resonator to detect point in time changes in volume of solution as well as analyte concentration in solution. However, the real benefit of the RF resonator lay in its potential ability to relay information about hydration states in real-time. In order to test this capability, a number of substances were left in contact with the TI Tag-It RFID – separated by a thin insulating layer of saran wrap – and the response of the resonator was measured over time. As water evaporated from the substances they effectively dehydrated, and the RF resonator should have recorded a corresponding frequency shift.

3.4.1 Silk Sponge Dehydration

The first set of materials tested were absorbing materials, including a polyacrylamide hydrogel and a silk sponge. Both of these substances were in consideration for inclusion as a wicking layer in the sweat patch prototype, and so were tested for their dehydrating and rehydrating properties. It soon emerged that the silk sponge was a clear front-runner, as the dehydration behavior of the polacrylamide hydrogel was monitored. Both were soaked in DI water and then left on the RF resonator to lose water. As seen in Figure 23, both the silk sponge and hydrogel took multiple hours to dehydrate a significant amount of DI water.

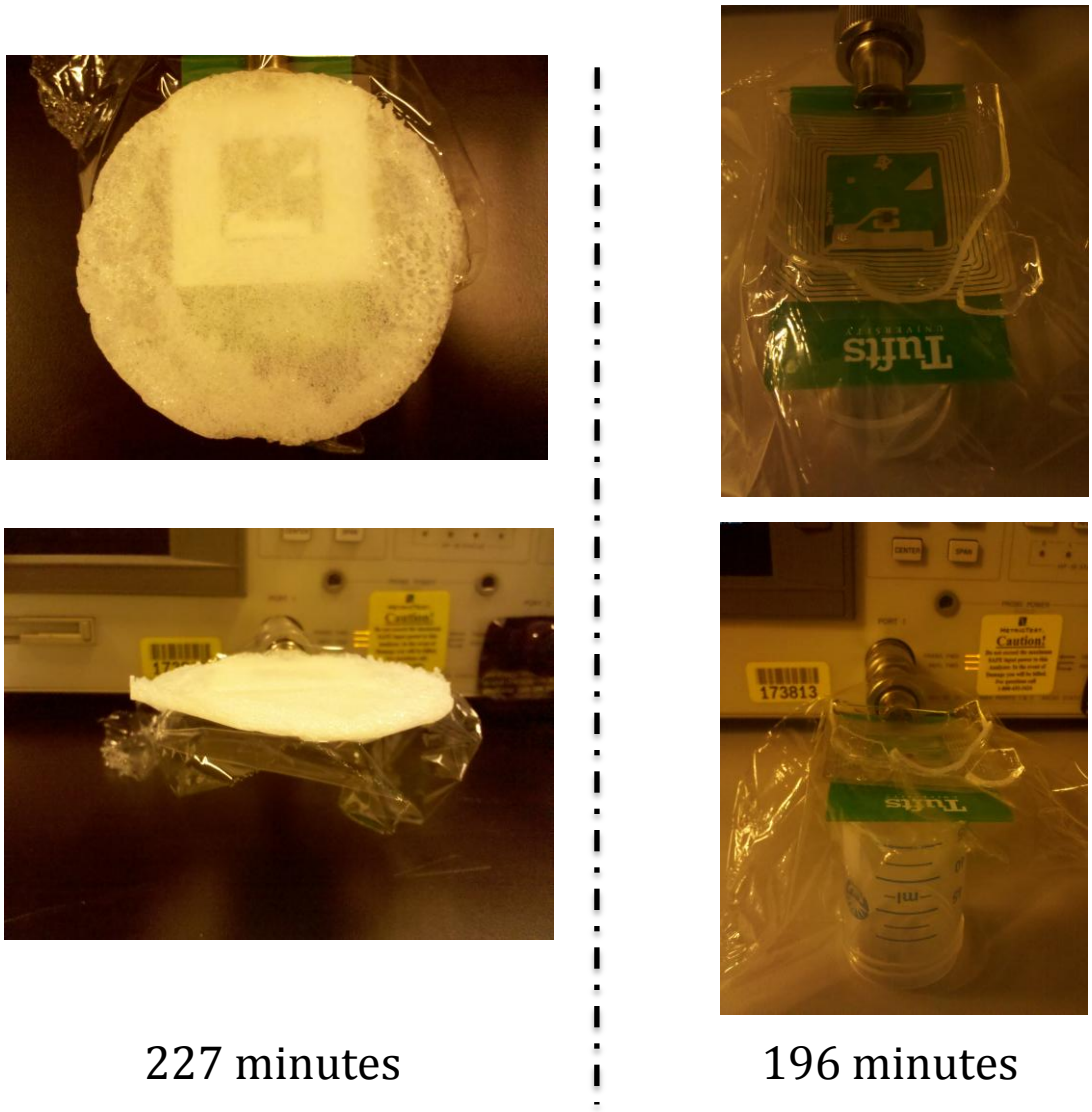

Figure 23: Comparison of dehydrated materials at similar time points– a silk sponge on the left and a polyacrylamide hydrogel on the right

However, the polyacrylamide hydrogel showed evidence of curling and cracking as it dried. The silk sponge on the other hand maintained shape and didn't shrink or deform as it lost fluid. This made the silk sponge a clearly superior wicking material, reinforced by the fact that the silk sponge was easily rehydrated while the polyacrylamide hydrogel was not. Figures 24 and 25 below show the frequency shift associated with a change in mass as measured by the amount of water lost.

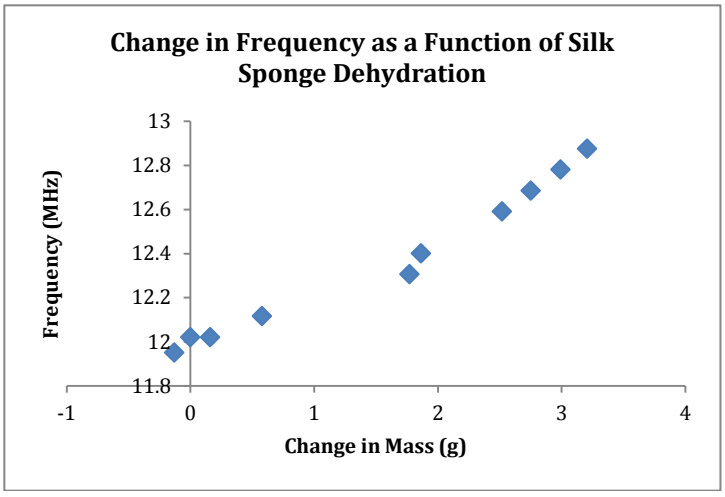

Figure 24: Frequency associated with amount of water lost in grams as a silk sponge dehydrates – Silk sponge Sample 1

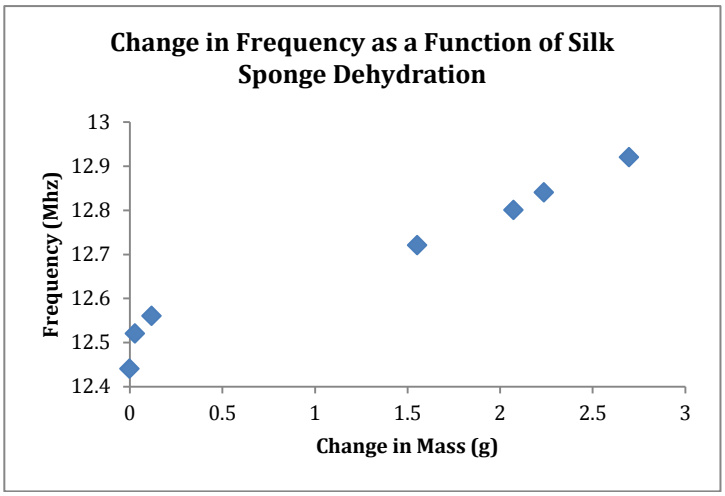

Figure 25: Frequency associated with amount of water lost in grams as a silk sponge dehydrates – Silk sponge Sample 2

The weight and frequency were simultaneously measured by using two similar silk sponges, one placed on a scale (measuring the change in weight) and the other on the RF resonator (measuring the change in frequency). With both silk sponge samples, there was a definitive increase in frequency as the sponge lost water and dehydrated.

3.4.2 Beef Tenderloin Dehydration

The dehydration experiment was repeated with a piece of beef tenderloin in order to simulate dehydration on the skin's surface and the parallel response of the RF resonator. Two similar pieces of beef were used, one on a scale to measure the weight of the beef as it dehydrated, and one on the RF resonator to determine if the frequency shifted as a result of the diminishing water content. Figure 26 shows the elapsed time of the water loss in the piece of beef on the scale, while Figure 27 correlates that weight loss to the frequency response measured on the HP 8753D

VNA. The results of the graph shown in Figure 26 were part of an experiment that was performed at a time when measurements were made manually. For this reason, data points were not necessarily taken at pre-determined intervals. This explains why there are some gaps in the time periods over which data was captured, for instance in the time interval from 150 to 250 minutes. In further dehydration experiments, an automated setup was developed that allowed for regular collection of data over pre-determined time intervals for the duration of the experiment.

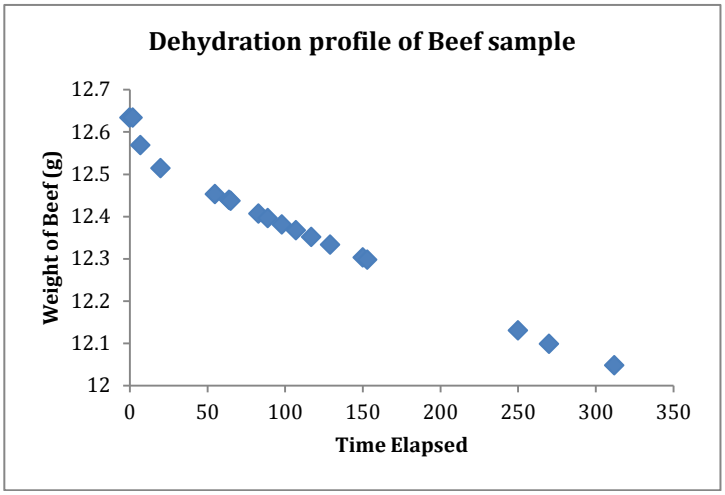

Figure 26: Water loss over time as measured by the weight of beef left to dehydrate in air

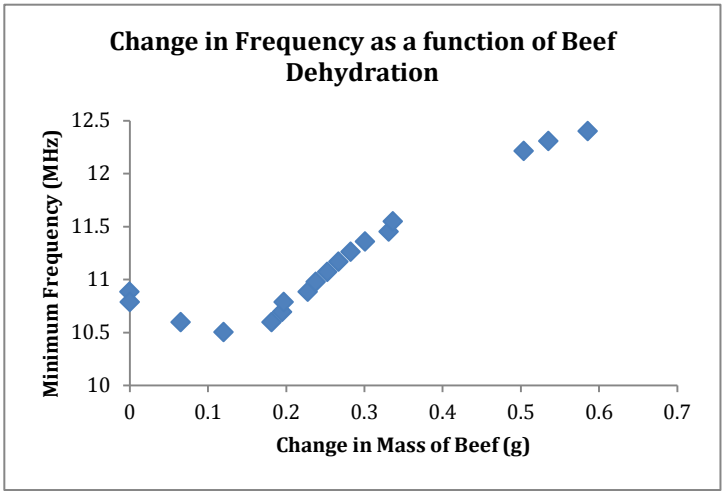

Figure 27: Frequency associated with amount of water lost in grams as a piece of beef tenderloin dehydrates in air

As with the silk sponge, there was a shift in frequency as the beef dehydrated over time. However, a similar trend was seen as in the measurements with the roast beef slice experiments, wherein the frequency initially decreased but then increased over time.

3.5 Sweat Collection Experiments

Though DPBS offered a useful sweat analog, it became apparent that testing with real sweat would be a necessary vetting process of determining the capabilities of the RF resonator as a sweat detection sensor.

3.5.1 Initial Human Testing

The first testing performed on humans involved a cellulose patch with no RF resonator affixed. Instead, a 5cmx5cm patch was placed on the back of a healthy, male subject using medical tape. Before placement of the patch, it was weighed and also placed on an RF resonator to ensure that it didn't cause a frequency shift. The RF resonator used for this experiment was the 13.56 MHz TI Tag-It RFID and measurements were made on the 8753D VNA. After the subject engaged in 30 minutes of vigorous exercise on a stationary bike, the patch was removed, weighed again, and placed on an RF resonator. The results of the measurements taken for two cellulose patch samples both before and after exercise can be seen in Table 12.1 and 12.2.

	Weight before (g)	Weight after (g)
Sample 1	2.006	3.063
Sample 2	3.078	4.182

(1)

	Freq. before (MHz)	Freq. after (MHz)
Sample 1	13.64	13.45
Sample 2	13.64	13.54

(2)

Table 12.1 & 12.2: (1) Measured weight (in grams) and (2) frequency response (in MHz) of two cellulose samples before and after absorbing sweat from the skin of a healthy, male subject after engaging in 30 minutes of exercise

If sweat is assumed to have similar properties to seawater, then the density of seawater can be used to translate grams of sweat accumulated in the patch to milliliters. At a conversion of 1.03 g/mL, each cellulose sample took up about 1mL of sweat. For this 1mL increase in sweat, there was an approximately 1% decrease in the measured frequency response of the RF resonator.

3.5.2 Sweat Patch Prototype Testing – Sweat Simulator

Before placing the sweat patch prototype on a human subject, the prototype was tested using the sweat simulator device. Driven by a syringe pump, the sweat simulator dispensed DI water in measured amounts. As the solution was dispensed onto the sweat patch, the response of the RF resonator on the opposite side of the sweat patch was measured. The sweat patch prototype was an all-in-one sensor, with an RF resonator designed to have a resonant frequency of about 410 MHz affixed to a cellulose patch. The frequency response of the sweat patch prototype in the sweat simulator is shown in Figure 28.

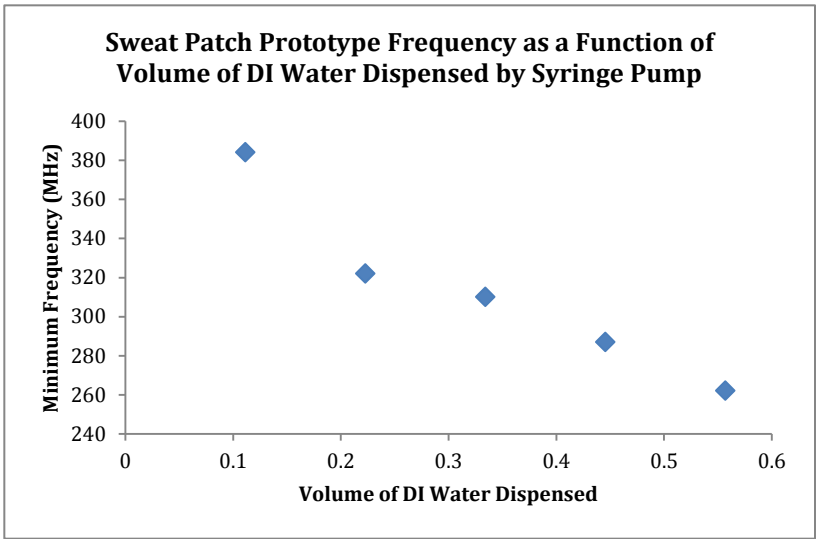

Figure 28: Frequency response of sweat patch prototype with gold RF resonator trace as DI water is dispensed via the sweat simulator syringe pump

The resonant frequency of the sweat patch prototype was higher than the TI Tag-It RFID resonator, and the frequency shift as a function of increasing DI water was more pronounced.

3.6 Android App

An Android software application was developed, in conjunction with an Android hardware accessory development kit, to detect the presence of a matched RF resonator tuned to 13.56 MHz. The ability to interface with mobile devices was a possibility because of the ability of the RF resonator to transmit information wirelessly. Modifications were made to an existing Android software application, known as the Basic Accessory Demo, to relay the strength of the coupling of the matched RF resonators to a mobile device – in this case a Samsung Galaxy tablet. The combination of a hardware created in lab to interface with the tablet, as well as modifications made to a software application, produced a working prototype of an RF resonance detector that interfaced with a mobile device.

3.7 Fabricated Resonators

A number of RF resonators at a variety of resonant frequencies were developed in lab. Table 13 outlines the different RF resonators as well as their measured resonant frequency.

RF Resonator Type	Resonant Frequency
Bob Melville's	13.54 MHz
Milled FR4/Copper Trace	13.56 MHz
Gold sputter coated on Tegaderm (150nm)	415 MHz
Gold sputter coated on Tegaderm (300nm)	415 MHz

Table 13: Measured resonant frequency for RF resonators fabricated in lab

Initially, RF resonators were milled from an FR4 substrate with a copper trace and were successful in resonating at the desired frequency. However, the need to work with a more conformal and comfortable interface necessitated fabrication of RF resonators on a different substrate. This is where Tegaderm was considered as a viable option, and as the results in Table 13 show fabrication on Tegaderm was possible.

3.8 Water Quality Testing

Sweat was not the only analyte targeted for detection by RF resonators during the course of the project. As the experiments progressed, the notion of using RF resonators as a measure of water quality emerged. Given that different brands of water have slightly different amounts of ions, drinking water became a logical substance to test.

A TI Tag-It RFID was put in contact with five different brands of drinking water, and the resulting shift in frequency can be seen in Figure 29 while the change in measured reflected power can be seen in Figure 30.

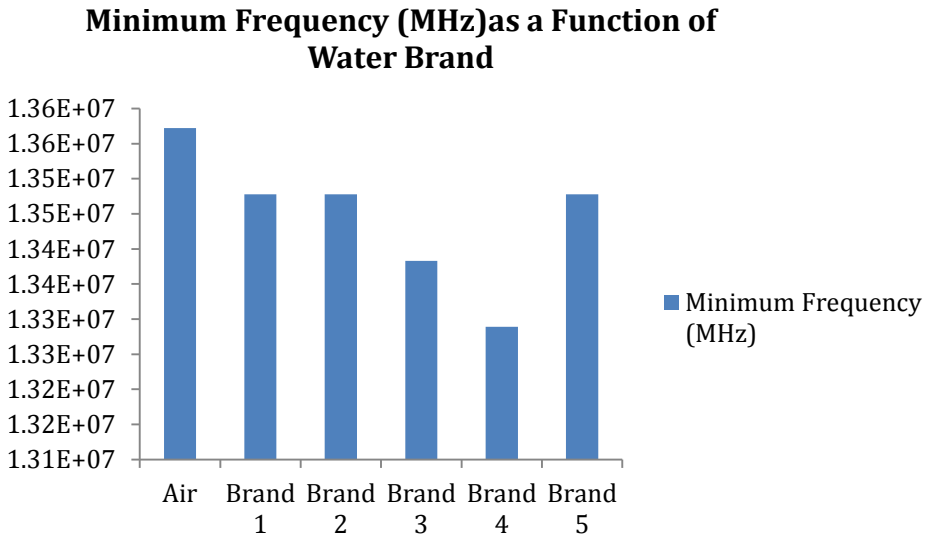

Figure 29: Frequency response of TI Tag-It RFID to different brands of drinking water

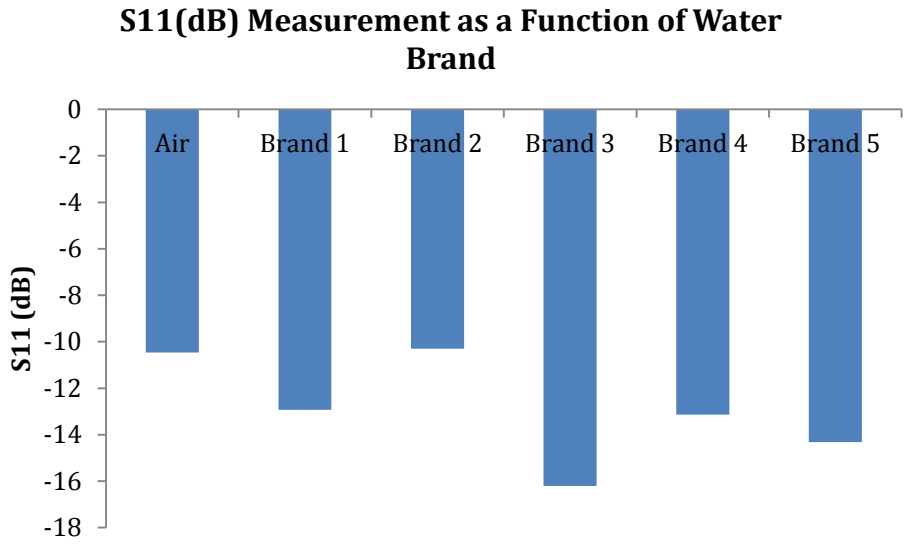

Figure 30: Change in measured reflected power of TI Tag-It RFID to different brands of drinking water.

The water was enclosed in a piece of acrylic with a circle cutout that held 5mL of liquid. A piece of saran wrap was placed over the cutout and held in place with double-sided cellotape. For each brand of drinking water, a unique signature was identified given the recorded frequency and reflected power response of the RF resonator.

4.Discussion

4.1 RF Resonator Performance

4.1.1 Sweat Volume Detection

The RF resonator sensing mechanism proved to be an indicator of overall volume of solution, whether DI water or another ionic solution was present. Given the clear difference in the dielectric constant of air and water, it's not surprising that the resonator had a marked response to the presence of water. The fabricated resonators might be better than the commercially produced RFID tags because of their intended purpose. RFID tags are designed and developed to operate at a specific resonant frequency and to perform within a narrow bandwidth, so they're literally made to resist changes in the surrounding environment. The substrate used to coat the RFIDs functions to safeguard the tag from outside elements, and some of the logic in the IC incorporated in the tag is to ensure that the resonant frequency doesn't deviate.

One of the design parameters of the fabricated resonators that could be improved upon is the insulating layer. In most of the experiments conducted in lab, this protective layer was saran wrap. It's not optimal to have saran wrap on sensors that have a potential future in the medical or athletic device market, as it's not a breathable material and could create a microclimate of unintended sweating. Tegaderm was explored as a replacement for saran wrap, but a full barrage of tests similar to the tests conducted with saran wrap need to be performed.

In general, the ability of the RF resonator to increasingly shift resonant frequency with the addition of solution substantiated the claim that it would work well as a sweat rate detector. The real-time capability of the sensor was put on display, and shows promise as a non-invasive sweat-monitoring tool.

4.1.2 Sweat Composition Detection

As a sweat composition detector, the RF resonator provided less conclusive results. While the response of the resonator changed in the presence of ionic solution, the sensitivity was harder to ascertain. Also, in order to detect a 1% decrease in body weight loss as sweat, the sensor would have to be able to distinguish 5mmol/L differences in sodium concentration. Though the RF resonator showcased the sensitivity to differentiate between 20mmol/L changes in sodium concentration, it didn't yet demonstrate the capability of going as low as 5mmol/L detection. That capability would have to be investigated further before moving forward with this sensing platform as a sweat composition detector.

A further design point to consider for the RF resonator being used as-is as a sweat composition device is it's innate inability to differentiate between concentrations of different ions. Though tests were only performed with NaCl and DPBS, prior work showed that the RF resonator is ion-agnostic (Potyrailo, 2010). Current sweat patches are analyzed in lab for the presence of a number of ions, including sodium, potassium and magnesium. One way to overcome that deficiency

would be to coat the resonator in a material that binds to an ion of interest and have a series of sweat patches that are each targeted for a specific ion. Another potential option is to measure a number of parameters (frequency, reflected power, and impedance) and enlist the help of Principal Component Analysis (PCA). A review of prior studies in the literature has shown the use of PCA to distinguish individual elements in a gaseous mixture through the processing capabilities of PCA (Potyrailo, 2011). This could be further extended in this sweat detection application to detect the levels of various ions in sweat.

For both the applications of sweat volume and composition detection, the RF resonator sweat patch prototype provided a set of results that are in line with the potential for a real-time, non-invasive hydration sensor. In an effort to make further gains on both fronts, the possibility of also making the sensor reusable or at least more than a one-time use application should be considered. Currently, the cellulose material used in the prototypes is not reusable after it has absorbed any type of liquid solution. The composition of the material is compromised as it warps slightly when wetted, similar to a piece of heavy-stock paper. A processed silk material, such as the silk sponges tested, could be a superior substitute. In the dehydration and rehydration testing, the silk sponges proved that they gain and lose fluid without conceding structural integrity. The silk sponges weren't used in the prototype development mainly because of the processing time required to create them, as opposed to the minimal time spent ordering cellulose samples. However, the material should be heavily considered for future iterations of the RF resonator sweat patch device.

4.2 Android App Development

In exploring options to interrogate and receive information about the response of the RF resonator to the surrounding environment in real-time, the Android development platform surfaced as a viable option. The open-source software environment and suite of software and hardware development tools contributed to the overall positive experience with the Android App development process. Figure 31 is a screen capture taken from the Samsung tablet that was used to test the Android app, and shows some of the potential ways to convey complex electromagnetic behaviors of an RF device in a user-friendly setting.

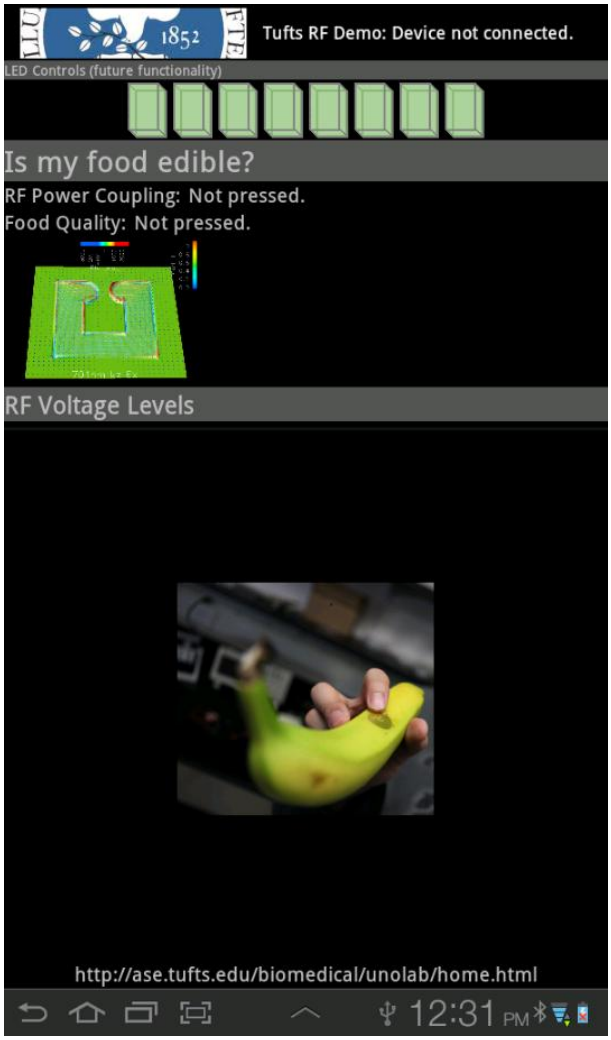

Figure 31: Screen capture of Android app modified for use as an RF detector

The app was developed with a food spoilage application in mind, but can be extended for use as a sweat detection application. In its current implementation, whenever an RF resonator with a matched frequency is placed in close proximity to the tablet, the application shown in Figure 31 will show a change in the RF voltage levels portion of the screen. The closer the RF resonator, the higher the RF voltage level displayed. This could be modified to act as a sweat volume and composition monitor, constantly monitoring the amount and type of sweat and alerting either the user or a health care provider or trainer when dehydration is imminent.

4.3 Future Directions

4.3.1 Integration with Mobile Devices

While the demonstration of the interaction between an RF resonator and a mobile device as shown in Figure 31 was interesting, the possibility of interfacing with these tablets and smart phones should be further explored. The possibility of developing a sweat patch that can relay information on a continuous basis to a

handheld device opens up a number of field applications for this sensing platform. A trainer could monitor the hydration state of an athlete during exercise, or a health care provider could keep an eye on the how dehydrated an elderly patient is in a non-invasive manner. An example of how to integrate this with the current sweat patch prototype is to place the prototype on the arm of the subject and then have a small mobile tablet strapped to the arm just over the patch. The mobile tablet device would be similar to mobile phones and mobile music players that runners sometimes affix to their arms to play music while they exercise. As the mobile device monitors the sweat volume and composition, it can relay that information to the subject, alerting them when to hydrate to avoid dehydration.

In order to the move forward with this mobile device application, the decision has to be made about what communication protocol to use. NFC is currently a popular choice for applications where the sensing device is close in proximity, while Bluetooth is making a play for the market with its low power offering. Additionally, Zigbee is another protocol utilized by some in the healthcare community to leapfrog information about many patients over a mesh network. As more devices come to market with wireless communication capabilities, and the benefits of NFC vs. BLE vs. Zigbee become more apparent, a clearer path will emerge.

In determining how to interface with mobile devices, in addition to the operating frequency, the placement of the sweat patch is important. Given the prevalence of mobile phones for use as music players during exercise in armbands, the arm is a potential spot for the patch. With the patch placed on the skin just under the mobile device that is fixed in an armband, the patch would be in close proximity to the mobile device and would be well positioned for measurements.

4.3.2 Multi-Sensor Array Network

Part of the complexity with monitoring dehydration is that the body responds in many different ways to the loss of fluids. While monitoring sweat rates and composition on the skin's surface in real-time fills an existing void in the hydration sensing market, the ability to simultaneously track multiple physiological markers would provide a more complete physiological picture. The idea is to attach an array of sensors in strategic locations throughout the body that each measure a relevant parameter and send all the information back to one centralized collection device. As the levels of elements such sweat volume, body temperature, pH, and hormone levels are collected; a more complete picture of the body's physiological response is created. Though this was not in the scope of this project, it was worth mentioning as a potentially impactful future direction.

4.3.3 Water Quality Monitoring

Also outside the initial scope of this project, but an interesting addendum to the sweat detection work, were the results obtained testing different brands of drinking water. The application for is for potential water quality monitoring; either in the reusable water bottles everyone carries around or in potentially compromised drinking water supplies in less-wealthy areas. Further testing would have to be performed in order to determine the response of the resonator to

bacteria cultures or other elements that are common in unsafe drinking water. However, the initial results from the preliminary testing with different brands of drinking water show the myriad sensing applications of the RF platform.

References

Armstrong, LE, et al., Urinary indices during dehydration, exercise, and rehydration, *International Journal of Sport Nutrition*, 8, 4, 345-55, 1998

Baker, Lindsay A., et al., Comparison of regional patch collection vs. whole body washdown for measuring sweat sodium and potassium loss during exercise, *Journal of Applied Physiology*, 107, 3, 887-895, 2009

Beasley, Jeffrey S., Modern Electronic Communication (9 ed.), pp4-5, 2008

Coyle, Edward E., Fluid and Carbohydrate Replacement During Exercise: How Much and Why?, *Hydration and Performance SSE #50, Gatorade Sports Science Library*, 1994

Heck, Howard, OGI EE564 website, Advanced Transmission Lines presentation, http://home.comcast.net/~howard.heck/, visited Fall 2011

Ivy, John, Portman, Robert, The Performance Zone, *Basic Health Publications*, 132 pages, 2004

Jefferies, D., The Smith Chart website, http://personal.ee.surrey.ac.uk/Personal/D.Jefferies/smith.html, visited Fall 2011

Kovacs, EM, et al., Urine color, osmolality and specific electrical conductance are not accurate measures of hydration status during postexercise rehydration, *Journal of Sports Medicine and Physical Fitness*, 39, 1, 47-53, 1999

Lavizzo-Mourey, Risa J., Dehydration in the Elderly: A Short Review, *Journal of the National Medical* Association, 79, 10, 1987

Lee, Youbok, RFID Coil Design, *Microchip Appnote AN678,* 1998

Makarov, N2PK developer, website http://www.makarov.ca/index.htm, visited Spring 2011-June 2012 sporadically

Maso, F., et al., Salivary testosterone and cortisol in rugby players: correlation with physiological overtraining items, *Br Journal of Sports Medicine*, 38, 260-263, 2004

Maughan, Ronald, et al., Rehydration and recovery after exercise, *SSE* #62, Volume 9, Number 3, 1996

Melville, Bob, RF Consultant, Spring 2011-June 2012, Personal conversations & Email

Mentes, Janet C., et al., Use of a Urine Color Chart to Monitor Hydration Status in Nursing Home Residents, *Biological Research for Nursing*, 7, 3, 197-203, 2006

Montgomery, Justin, iPhone 4S Bluetooth 4.0 Capability More Beneficial for mHealth than NFC?, *mHealthWatch blog,* http://mhealthwatch.com/iphone-4s-bluetooth-4-0-capability-more-beneficial-for-mhealth-than-nfc-17855/, visited Spring 2012

Morgan, R.M, Patterson, M.J., and M.A. Nimmo. 2004. Acute effects of dehydration on sweat composition in men during prolonged exercise in the heat. *Acta Physiol Scand*, 182: 37-43

Palaciosa, C., Sweat mineral loss from whole body, patch and arm bag in white and black girls, *Nutrition Research*, 23, 3, 401-411, 2003

Peak Performance, website, http://www.pponline.co.uk/, visited Fall 2011

Potyrailo, R.A., Monk, D., et al. Integration Of Passive Multivariable RFID Sensors Into Single-Use Biopharmaceutical Manufacturing Components. *IEEE RFID*, 1-7, 2010

Potyrailo, Radislav, Selective Vapor Monitoring Using Individual Multivariable RFID sensors, *Olfaction and Electronic Nose: Proceedings of the 14th International Symposium on Olfaction and Electronic Nose*, AIP Conf. Proc. 1362, pp.35-36, 2011

Potyrailo, Radislav, Personal conversations at 2012 IEEE RFID conference in Orlando, FL, April 2-4, 2012

Raff, Hershel, et al., New Enzyme Immunoassay for Salivary Cortisol, *Clinical Chemistry*, 49, 1, 203-204, 2003

Reeder, Nick, EET 155 website, Source of RLC Figure, http://people.sinclair.edu/nickreeder/eet155/mod06.htm, visited Fall 2011

Robbins, Allan H., Miller, Wilhelm C., Circuit Analysis Theory and Practice, *Delmar Cengage Learning*, 2000

Rockwood, Danielle N. et al, Materials fabrication from Bombyx mori silk fibroin, *Nature Protocols*, 6, 1612-1621, 2011

Sample, Alanson, et al., Analysis, Experimental Results, and Range Adaption of Magnetically Coupled Resonators for Wireless Power Transfer, *IEEE*, 2010

Shelton, Andy, Trainer for Leicester Tigers Rubgy Club, Skype conversations, June 2011-June2012, monthly

Simerville, Jeff A., et al., Urinalysis: A Comprehensive Review, *American Family Physician*, 71, 6, 1153-1162, 2005

UK RFID, Informational website, http://ukrfid.com/hardware/rfid_tags, visited Fall 2011

Yeargin, Susan Walker, et al., Thermoregulatory Responses and Hydration Practices in Heat-Acclimatized Adolescents During Preseason High School Football, *Journal of Athletic Training*, 42, 2, 136-146, 2010